Redistribution of centrosomal proteins by centromeres and Polo kinase controls nuclear envelope breakdown

Andrew J. Bestul[1], Zulin Yu[1], Jay R. Unruh[1] and Sue L. Jaspersen[1,2]

[1] Stowers Institute for Medical Research, Kansas City, MO

[2] Department of Molecular and Integrative Physiology, University of Kansas Medical Center, Kansas City, KS

Running Title: Centrosomal control of NEBD

Corresponding author:

Sue L. Jaspersen

E-mail: slj@stowers.org

Keywords: nuclear envelope breakdown, Polo kinase, LEM domain, Sad1-UNC-84 domain, spindle pole body

Characters: 36,795

Summary

Nuclear envelope breakdown is necessary for fission yeast cells to go through mitosis. Bestul et al. show that the SUN protein, Sad1, is vital in carrying out this breakdown and is regulated by the centromere and Polo kinase.

Abstract

Proper mitotic progression in *Schizosaccharomyces pombe* requires partial nuclear envelope breakdown (NEBD) and insertion of the spindle pole body (SPB – yeast centrosome) to build the mitotic spindle. Linkage of the centromere to the SPB is vital to this process, but why that linkage is important is not well understood. Utilizing high-resolution structured illumination microscopy (SIM), we show that the conserved SUN-protein Sad1 and other SPB proteins redistribute during mitosis to form a ring complex around SPBs, which is a precursor for NEBD and spindle formation. Although the Polo kinase Plo1 is not necessary for Sad1 redistribution, it localizes to the SPB region connected to the centromere, and its activity is vital for SPB ring protein redistribution and for complete NEBD to allow for SPB insertion. Our results lead to a model in which centromere linkage to the SPB drives redistribution of Sad1 and Plo1 activation that in turn facilitate NEBD and spindle formation through building of an SPB ring structure.

Introduction

Microtubule-organizing centers (MTOCs) are found throughout eukaryotes and carry out a vast array of cellular processes, including microtubule nucleation (Bettencourt-Dias and Glover, 2007; Wu and Akhmanova 2017; Kollman et al 2011). During mitosis, MTOCs known as the centrosome (metazoans) or spindle pole body (SPB, fungi) serve as the poles of the mitotic spindle as part of the spindle apparatus that facilitates accurate chromosome segregation. Failure of the centrosome to properly assemble the mitotic spindle results in chromosome missegregation and genomic instability (Nigg 2002; Ganem et al. 2009; Gönczy et al. 2015). In metazoans and in the fission yeast, *Schizosaccharomyces pombe*, the centrosome/SPB is located on to cytoplasmic surface of the nuclear envelope (NE) throughout interphase. As cells enter mitosis, nuclear envelope breakdown (NEBD) begins beneath the centrosome/SPB. In contrast to the complete NEBD of most metazoan cells, fission yeast restricts NEBD to the region localized only underneath SPB. This partial NE fenestration allows for SPB insertion into the nuclear membrane, which enables microtubules to access chromosomes to create the mitotic spindle (Ding et al 1997; Uzawa et al 2004; Cavanaugh and Jaspersen 2017). Partial NEBD is also observed in *Caenorhabditis elegans* early embryos and in the syncytial embryonic division cycles of *Drosophila melanogaster* (Hachet et al. 2007; Portier et al. 2007; Paddy et al. 1996).

A major unresolved question is how NEBD is spatially regulated in cells that undergo partial NEBD. This question has been most extensively studied in fission yeast meiosis where the linkage of a cluster of telomeres (called the telomere bouquet) to SPB

through the NE is vital to trigger NEBD and spindle formation (Tomita and Cooper, 2007; Klutstein and Cooper, 2014). The SPB receptor for telomeres during meiosis is the LINC (Linkage of Nucleoskeleton and Cytoskeleton) complex, composed of the outer nuclear membrane (ONM) KASH-domain protein Kms1 and the inner nuclear membrane (INM) SUN-domain protein, Sad1. Telomeric linkage to the LINC is achieved by association of the meiosis-specific telomere-binding proteins Bqt1 and Bqt2 with Sad1 (Chikashige et al., 2006). Spatialized NEBD at the SPB is also regulated by chromosome-NE association in mitotic cells. Here, the meiosis-specific INM KASH-protein Kms1 is replaced by its mitotic ortholog Kms2 (Wälde and King, 2014; Bestul et al., 2017). Also, the telomere bouquet is replaced by centromeres, which are clustered underneath the SPB during interphase of mitotic cells through association of the mitotic centromere binding protein Csi1 with Sad1 (Funabiki et al., 1993; Hou et al., 2012). However, loss of Csi1 only partially disrupts Sad1-centromere linkage, implicating other unknown linkage factors such as the LEM-domain proteins Lem2 and/or Man1 that also bind to centromeres/telomeres (Hiraoka et al., 2011; Steglich et al., 2012). A single centromere bound to the LINC complex is sufficient for proper spindle formation; in *sad1.2*, which displays a partial loss of centromere-binding function, only cells with an unattached centromere have a defect in mitotic progression (Fennell et al., 2015; Fernandez-Alvarez et al., 2016). Analysis of *sad1.2* showed a defect in NEBD, providing evidence that chromosome linkage via the LINC complex regulates partial NEBD at mitotic entry. How a chromosome-NE linkage leads to NEBD and SPB insertion is unknown, although it is thought that chromatin might help increase the localize critical

mitotic regulators to the SPB to bring about NE remodeling (Fernandez-Alvarez et al., 2016).

In *Saccharomyces cerevisiae*, the SPB is inserted into the NE by the spindle pole insertion network (SPIN), which includes the Sad1 homolog, Mps3, and its binding partner, Mps2 (Rüthnick et al., 2017; Chen et al., 2019). The SPIN forms a donut-like structure that anchors the SPB in the NE. Like Mps3, Sad1 also localizes to a ring-like structure around duplicated SPBs at mitotic entry (Bestul et al., 2017). To investigate the link between Sad1 ring formation, centromere linkage and association with other mitotic regulators, we used high-resolution structured illumination microscopy (SIM) to study Sad1 reorganization along with that of Kms2, the mitotic regulator Cut12 and Cut11, a dual component of SPBs and nuclear pore complexes (NPCs). All proteins form a ring-like structure that is Sad1 and centromere-dependent. We further show that Polo kinase (*plo1*+) is critical for ring formation and NEBD. Taken together, our data shows that the centromere-LINC linkage is necessary to drive proteins into a mitotic SPB ring structure that allows for NEBD and SPB insertion.

Results

Identifying components of the fission yeast mitotic SPB ring

Previously, we examined Sad1 localization using SIM in cells arrested at G2/M using the *cdc25.22* mutant (Bestul et al., 2017). We found images in which Sad1-GFP shifted from underneath the duplicated side-by-side SPBs to a full or partial ring surrounding the SPB core. This ring-like pattern of localization is reminiscent of Mps3 in budding yeast, which like other SPIN components, surrounds the SPB core (Chen et al., 2019).

To identify other SPB proteins that redistribute into a ring like Sad1, we introduced fifteen previously GFP-tagged SPB components as well as Cut11-GFP into a *cdc25.22* strain containing Ppc89-mCherry to mark the SPB core. Cells were arrested at G2/M at 36°C for 3.5 h then were released into mitosis by shifting to 25°C. Examination of cells at 0, 10, 20 and 30 min allowed us to follow ring formation and SPB insertion upon mitotic entry. Critically, Ppc89-mCherry and other components of the SPB core (GFP-Pcp1, Cam1-GFP, Sid4-GFP, Cdc11-GFP, Mto1-GFP) appeared as two foci at all time points, indicating that the SPB core does not reorganize upon entry into mitosis (Bestul et al., 2017). Electron microscopy (EM) shows that the laminar core is simply lowered into a fenestrated region of the NE during mitosis (Ding et al., 1997; Uzawa et al., 2004).

Four proteins redistributed into ring-like structures: Sad1, Kms2, Cut12 and Cut11 (Fig 1A). Sad1 and Cut11 rings are robust, encompassing almost the entire perimeter of duplicated SPBs, while Cut12 and Kms2 only form partial rings. Cut11 and Kms2

localization to the region surrounding the SPB is not unexpected as both contain transmembrane domains and are orthologous (Cut11) or similar (Kms2) to the SPIN components Ndc1 and Mps2 that distribute around the SPB in budding yeast. However, Cut12 does not have a budding yeast ortholog and it lacks a transmembrane domain. We hypothesize that Cut12 is targeted to a ring through its interaction with Kms2 in much the same way that the soluble protein Bbp1 is targeted to the SPIN by Mps2 (Wälde and King, 2014; Kupke JBC 2017; Schramm EMBO J 2000). Kms2-dependent Cut12 targeting could explain why these rings are similar in appearance but different than Sad1 and Cut11.

Analysis of Sad1, Kms2 and Cut12 distribution following release from *cdc25.22* suggests a temporal order of reorganization and recruitment that can be divided into four distinct steps: 1) in G2/M, SPBs are in a side-by-side configuration with protein present at or between the SPBs; 2) as cells enter into mitosis, a single ring is observed; 3) later, the ring encompass both SPBs forming a double ring; 4) finally, as SPBs separate, a ring surrounds each of the two SPBs (Fig 1A).

Stepwise formation of the SPB ring is initiated by Sad1

To determine if a temporal hierarchy exists in formation of the rings, we quantitated the fraction of cells containing at least one observable ring at 10 min after *cdc25.22* release. At this timepoint, 89.5% of Sad1 had redistributed to a ring, compared to 77.5% of Kms2 and 63.4% of Cut12 (Fig 1B). In addition, 36.9% of the Sad1 rings were in the more mature double ring conformation at this time, compared to 19.2% of Kms2 and

Figure 1

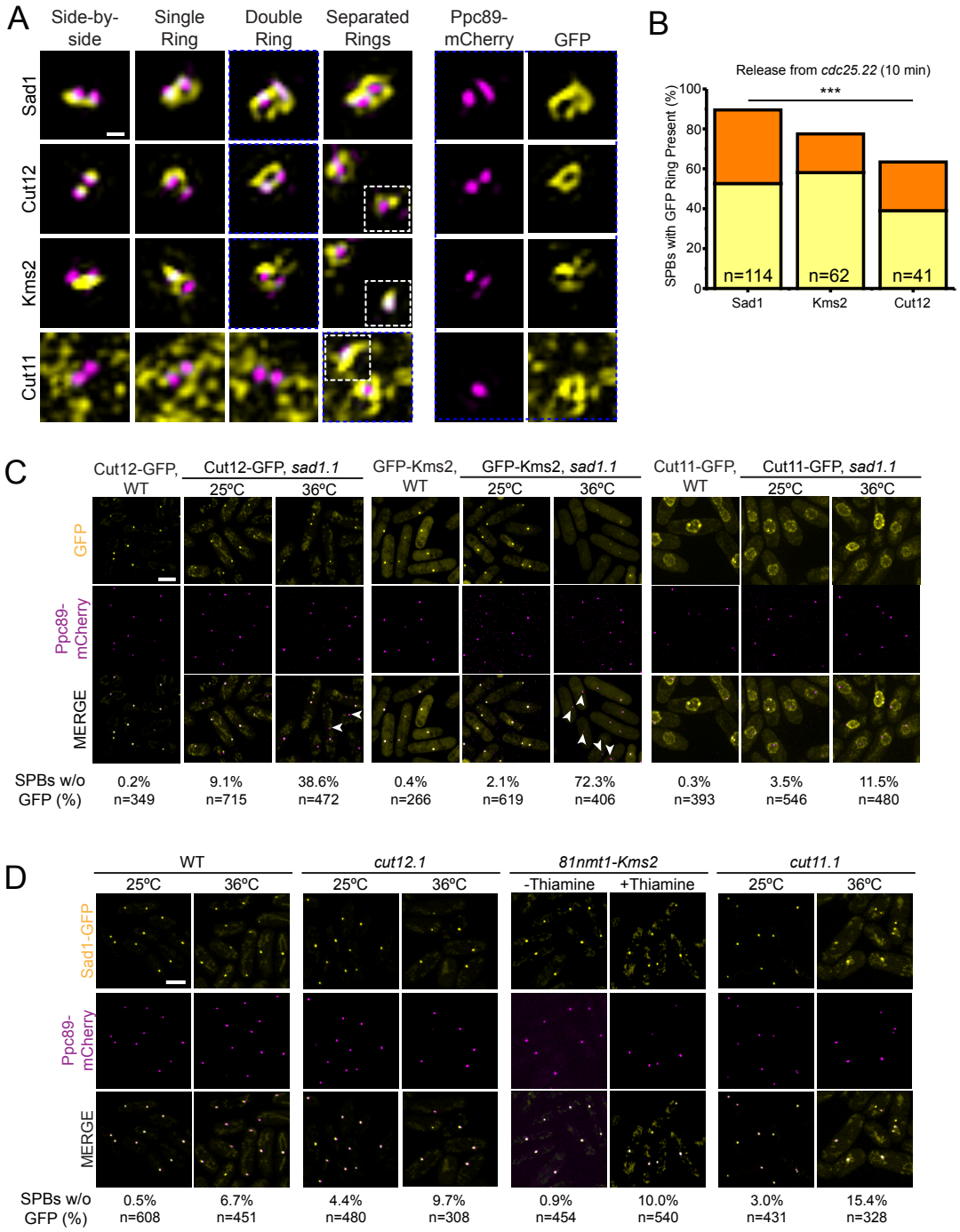

Figure 1. Four SPB proteins constitute the Sad1-dependent *S. pombe* mitotic SPB ring. (A-B) *cdc25.22* cells containing Ppc89-mCherry and the indicated GFP-tagged SPB components were arrested in late G2 by growth at 36°C for 3.5 h, then released into mitosis by shifting back to 25°C. Samples were taken at 0, 10, 20 and 30 min for analysis by SIM. (A) Sad1-GFP, Cut12-GFP, GFP-Kms2 and Cut11-GFP (yellow) redistribute relative to the SPB (magenta) as cells enter mitosis. At the arrest, SPB rings

have not formed (side-by-side); next, a single ring is observed; followed by a double ring that encapsulates both SPBs; finally, separated rings are observed as the poles move apart (one SPB in the same cell is shown as inset, white boxes). Individual channels of the double ring or separated rings are shown on the right, indicated by blue boxes. Bar, 200 nm. (B) Percentage of SPBs containing single (yellow) and double (orange) rings of the indicated protein was quantitated at 10 min after *cdc25.22* release. Cut11-GFP does not localize to the SPB at this time point so it was not included. ***, p=0.0013 based on χ^2 test. (C) Confocal images from wild-type or *sad1.1* containing Ppc89-mCherry (magenta) and the indicated GFP-tagged SPB component (yellow) grown at 25°C or shifted to 36°C for 3.5 h. Bar, 5 µm. Percentage of SPBs with no or very weak associated GFP signal (Examples indicated by arrowheads) is indicated below each corresponding column along with the number of SPBs analyzed (n). (D) Confocal images from *cut11.1* and *cut12.1* strains containing Sad1-GFP (yellow) and Ppc89-mCherry (magenta) grown at 25°C or shifted to 36°C for 3.5 h, and from *81nmt-HA-Kms2* cells with Sad1-GFP (yellow) and Ppc89-mCherry (magenta) grown in the absence or presence of 20 µM thiamine for 16 h. Bar, 5 µm. Percentage of SPBs without Sad1-GFP signal is indicated below each corresponding column along with the number of SPBs analyzed (n).

24.4% of Cut12. This suggests that Sad1 reorganization precedes that of Cut12 and Kms2. Cut11-GFP did not localize to the SPB until mitosis and only appeared in a ring ~30 min after *cdc25.22* release at or near the time of SPB separation. In a few rare cases, we observed Cut11-GFP double ring structures, but most were separated rings. From this data, we propose a temporal order of ring formation that starts with Sad1, followed by Kms2 and Cut12 and then finally Cut11 right before SPB separation.

Based on our temporal model of ring assembly, Sad1 serves as the gatekeeper and loss of *sad1+* function should lead to defects in redistribution of other components. Indeed, in *sad1.1* at 36°C, 38.6% did not contain Cut12-GFP compared to 0.2% of wild-type cells grown at the same temperature. More strikingly, 72.3% of *sad1.1* compared to 0.4% of wild-type cells lost GFP-Kms2 at 36°C. However, Cut11-GFP SPB localization was only modestly affected in *sad1.1* (Fig 1C). This suggests that Sad1 regulates the SPB localization and therefore the ring distribution of Kms2 and Cut12 but points to a Sad1-independent mechanism of Cut11 localization and ring formation, possibly through NE diffusion (West et al., 1998).

As the gatekeeper, we would also predict that Sad1 redistribution to a ring would be unaffected by loss of function in the downstream components. Sad1-GFP strains are slightly temperature sensitive and thus at 36°C in wild-type cells, 6.7% of SPBs lost the Sad1-GFP signal. The fraction of cells lacking Sad1-GFP at the SPB increased a small amount in *cut12.1* (9.7%) and *81nmt1-HA-Kms2* (10.0%), but this change is not statistically significant (Fig 1D). Thus, loss of Cut12 or Kms2 do not affect Sad1

localization. In *cut11.1* at 36°C, 15.5% of SPBs lacked Sad1-GFP – over twice the amount of wild-type cells (Fig 1D). It is unclear if Cut11 is needed for Sad1 localization per se, or if the detachment of SPBs from the NE that specifically occurs in the *cut11.1* strain contributes to Sad1 loss from the SPB as the poles are not embedded in the NE (West et al., 1998). Together, these data support our model that Sad1 is the first protein the redistribute to a ring at the fission yeast SPB and its relocalization is needed for Cut12 and Kms2 ring formation. Cytological and genetic data showed that Sad1 interacts with both Kms2 and Cut12 (Walde and King 2014; Miki et al., 2004). Although Sad1 also interacts with Cut11 in the yeast two hybrid system (Varberg et al., 2020), no physical interactions between Cut11 and ring components have been reported in fission yeast, supporting the possibility of an independent recruitment pathway.

Formation of the mitotic ring coincides with NEBD

The appearance of Sad1, Kms2, Cut12 and Cut11 in ring-like structures coincides with the timing of SPB insertion, which requires creation of the NE pore known as a fenestra. In wild-type cells, a small part of the NE is broken down and is quickly plugged by the SPB, keeping the NE intact during mitosis. Using *nmt3x-NLS-GFP* to monitor nuclear integrity, an NLS-GFP reporter remains in the nucleus at all times in wild-type cells (Fernandez-Alvarez et al., 2016). If SPB insertion is disrupted (*brr6.ts8*), large holes in the NE form (Tamm et al., 2011) and the ratio of nuclear to cytoplasmic (N:C) GFP of the reporter decreases (Fig 2A).

If the mitotic ring is involved in NEBD, it seemed likely that blocking ring assembly by mutation of *sad1*+, *kms2*+, *cut12*+ or *cut11*+ might uncouple fenestration and SPB insertion, leading to alterations of NE integrity. Analysis of *nmt3x-NLS-GFP* in *sad1.1, cut12.1, cut11.1* and *81nmt1-HA-Kms2* showed a range of phenotypes that can be categorized as: 1) severe/complete loss of NE integrity, 2) partial loss of NE integrity and 3) no loss of NE integrity (Fig 2B). Similar to the *brr6.ts8* (N:C 1.4±0.1) mutant, *cut11.1* (N:C 1.5±0.1) showed complete loss of NE integrity. *cut12.1* and *81nmt-HA-Kms2* showed a partial loss of NE integrity with N:C ratios of 2.2±0.1 and 2.3±0.1 under non-permissive conditions. While it is possible that the decrease in *81nmt-HA-Kms2* is partially due to repression of the NLS-GFP promoter, which is also thiamine-repressible, the differences in promoter strengths (strong *nmt3x* vs. weak *81nmt1*) allowed us to get significant results that are likely due to loss of *kms2*+ function rather than the NLS-GFP. Even at restrictive conditions, the N:C ratio for *sad1.1* remained high (9.5±0.3), similar to wild-type cells (10.2±0.3). These results suggest that *sad1*+ function is required for NEBD. Without Sad1, other components do not localize and thus further steps leading to NEBD cannot occur. Cut12, Kms2 and Cut11 are not required to initiate NEBD as partial or total loss of NE integrity occurs in their absence. However, NEBD and SPB insertion are uncoupled in the mutants (Tallada et al., 2009; West et al., 1998; Walde and King, 2014).

Figure 2

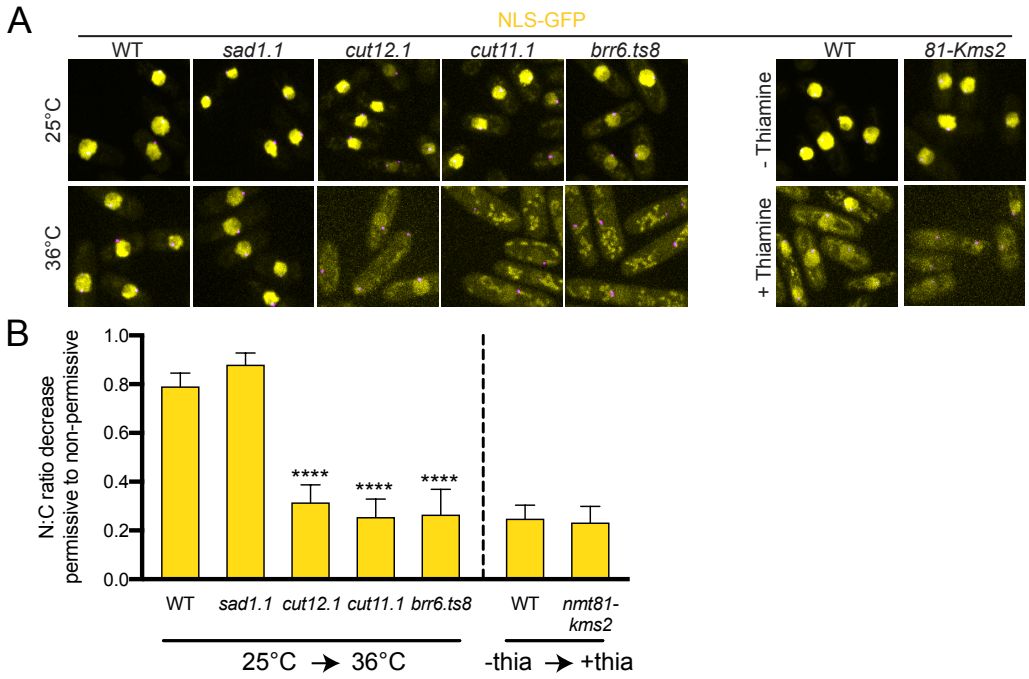

Figure 2. Nuclear integrity is maintained in the absence of *sad1+* function. The soluble nuclear reporter 3nmt-NLS-GFP was introduced into wild-type and mutant strains to test NE integrity. Cells were grown at 25°C or shifted to 36°C for 3.5 h (for wild-type; *sad1.1, cut12.1, cut11.1* and *brr6.ts8*) or grown for ~16 h in the absence or presence of 20 μM thiamine (for WT and *81nmt-HA-Kms2*). (A) Representative confocal images. Bar, 5 μm. (B) The ratio of total nuclear (N) to cytoplasmic (C) GFP fluorescence was determined for each strain and a normalized ratio based on the permissive condition was determined. Plotted is the decrease of each N:C ratio when going from the permissive condition (25°C or no thiamine) to the restrictive condition (36°C or 20 μM thiamine). A value of 1.0 would indicate no decrease between the two conditions. Errors bars, SEM. ****$p<0.001$, based on χ^2 test compared to wild-type. n=100.

Centromeric-SPB linkage proteins Lem2 and Csi1 contribute to Sad1 redistribution into the mitotic SPB ring

As the gatekeeper whose function is needed to trigger NEBD, we were interested in determining how Sad1 is regulated. Sad1 redistribution typically begins by the formation of a small single ring, which we assumed surrounded either the 'old' SPB present from the previous cell cycle or the 'new' SPB formed by SPB duplication. Detailed inspection of the Sad1-GFP single ring showed it often formed between the two SPBs under the bridge region (18/38; non-SPB), rather than surrounding one of two SPBs (20/38; SPB) (Fig S1A). This suggests that the Sad1 redistribution is not linked to the SPB per se but to extrinsic landmarks, such as the centromere that is attached to the SPB through a Sad1-based LINC complex (Fernandez-Alvarez et al., 2016). Consistent with this idea, we observed that the Sad1 rings co-localized with the centromere, which was marked with Mis6-GFP (Fig S1B).

The coincidence of Sad1 rings with the centromere suggested that centromeric proteins might regulate Sad1 redistribution. Two candidates stood out as possible regulators: Csi1, a Sad1-interacting protein whose loss leads to partial disruption of the centromere-SPB linkage (Hou et al., 2012); and Lem2, which localizes to the SPB throughout interphase and early mitosis (Hiraoka et al., 2011), binds to chromatin near the centromere and functions in NE reformation (Gu et al., 2017; Barrales et al., 2016; Banday et al., 2016). Also, the double deletion of *csi1*Δ*lem2*Δ leads to loss of centromere-SPB linkage and subsequent loss of mitotic spindle formation (Fernandez-Alvarez and Cooper 2017). At high resolution, both Csi1-GFP and Lem2-GFP formed

ring-like structures, similar to Sad1-GFP (Fig 3A, S2A). Single particle averaging (SPA) using Ppc89-mCherry as a fiducial marker allowed us to align SPBs to determine the average protein distribution around the pole for multiple SIM images. This showed that Csi1-GFP had a ring with a diameter similar to Sad1-GFP while Lem2-GFP rings were typically larger (Fig 3A, S2A).

Co-localization of Csi1-GFP and Sad1-mCherry in synchronized cells (using *cdc25.22*) confirmed the size similarity between Csi1 and Sad1 rings and further showed that both proteins re-distribute with the similar timing (Fig 3B). Furthermore, *sad1.1* loss-of-function specifically blocked Csi1 ring formation (Fig 3C). In contrast, we found that Lem2-GFP localizes to rings in both interphase and early mitosis prior to SPB separation (signified by Cut11-GFP ring formation) (Fig S2B). Lem2-GFP ring formation was also impaired in a *sad1.1* background (Fig S2C), suggesting that Sad1 is required to stabilize the Lem2 ring structure or that at the arrest, Lem2 has begun its disassembly. The size, timing and Sad1-dependence of Csi1 localization are consistent with a direct role for Csi1 in Sad1 ring formation and mitotic progression. While Lem2 may also be involved, the size of the Lem2 ring relative to Sad1 and the predominant interphase pattern would suggest an indirect role (see Discussion).

To determine if Csi1 regulates Sad1, we examined the distribution of Sad1-GFP in *csi1Δ* and *lem2Δ csi1Δ* backgrounds in normal (25°C) and stressed (36°C) conditions. As a control, we also examined Sad1-GFP in other deletion strains for proteins involved in centromere or NE-binding and/or NE reformation: Lem2, Nur1 (Banday et al., 2016);

Figure 3

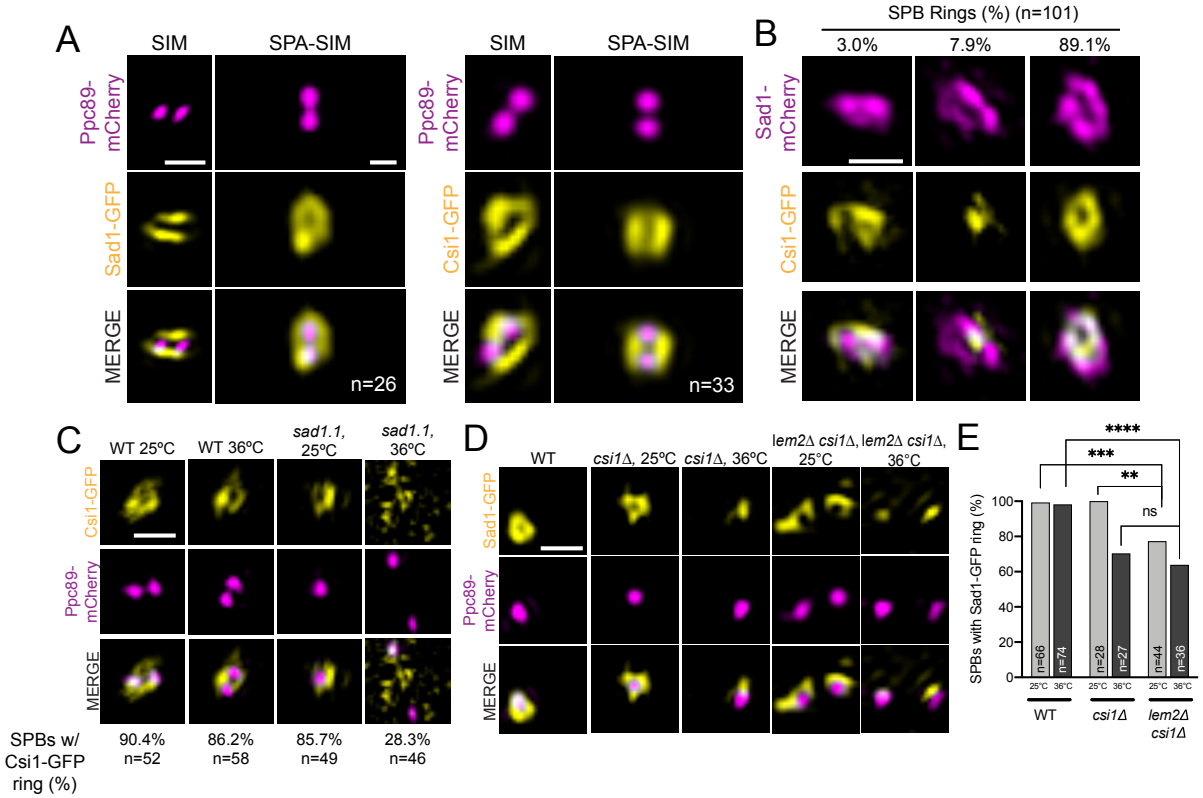

Figure 3. Centromeric protein Csi1 regulates Sad1 mitotic SPB ring formation and also forms a mitotic SPB ring. (A) Individual SIM images of *cdc25.22* arrested cells containing Sad1- or Csi1-GFP (yellow) and Ppc89-mCherry (magenta) (left columns). Single particle averaging (SPA) was used to combine the indicated (n) number of individual SIM images (right columns). Bar, 500 nm. (B) SIM images of Sad1-mCherry (magenta) and Csi1-GFP (yellow) in *cdc25.22* arrested cells that were then released at 25°C for 10 min before imaging. Three configurations were observed in the indicated fraction of cells: Csi1 ring with no Sad1 ring (left), Sad1 ring with no Csi1 ring (center), and rings of both Sad1 and Csi1 (right). n=101. Bar, 500 nm. (C) SIM images of Csi1-GFP (yellow) and Ppc89-mCherry (magenta) in wild-type and *sad1.1* backgrounds, grown as described in Fig 1D. The percentage of cells containing a ring of Csi1-GFP around the SPB was determined for each based on the indicated number of cells (n). (D-E) Wild-type, *csi1Δ* or *lem2Δ csi1Δ* cells with Sad1-GFP (yellow) and Ppc89-mCherry (magenta) were grown for 4 h at 25°C or 36°C and then imaged. (D) Representative SIM images. (E) Percentage of SPBs with a Sad1 ring. P values were determined using the χ^2 test, ns=not significant; **p=0.028; ***p=0.0056; ****p<0.001. Bars, 500 nm.

Figure S1

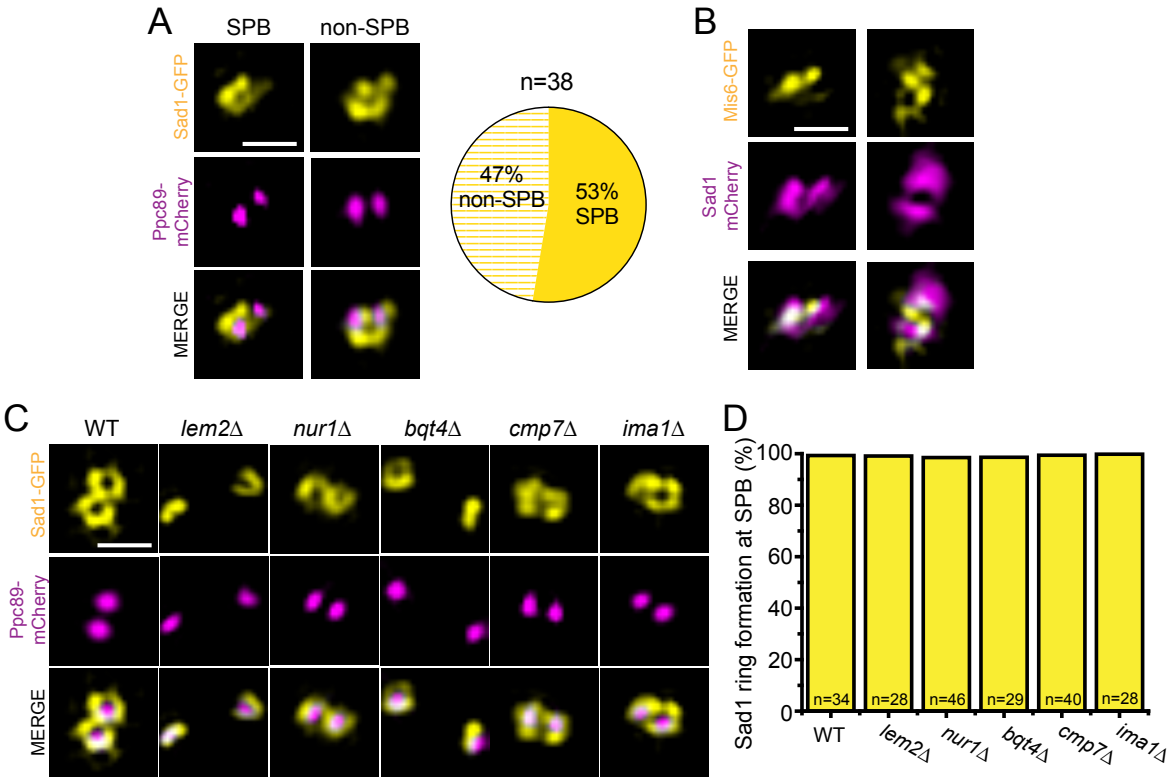

Figure S1. Sad1 ring formation is co-incident with the centromere. (A) *cdc25.22* cells containing Ppc89-mCherry (magenta) and Sad1-GFP (yellow) were grown for 3.5 h at 36°C and then released to 25°C for 10 min before imaging by SIM. The Sad1-GFP single ring co-localized with the SPB (left) or to an area in between the two SPBs (right, non-SPB). The percentage of cells in each configuration is shown. (B) Similarly, *cdc25.22* cells with Sad1-mCherry (magenta) and Mis6-GFP (yellow) were arrested and released to determine the position of the centromere relative to the Sad1 ring. (C-D) *cdc25.22* cells containing Ppc89-mCherry (magenta) and Sad1-GFP (yellow) in the indicated centromere/INM protein deletion background were arrested at the G2/M boundary and analyzed by SIM. (C) Representative SIM images. (D) Percentage of mitotic SPBs that had Sad1-GFP rings. Bars, 500 nm.

Figure S2

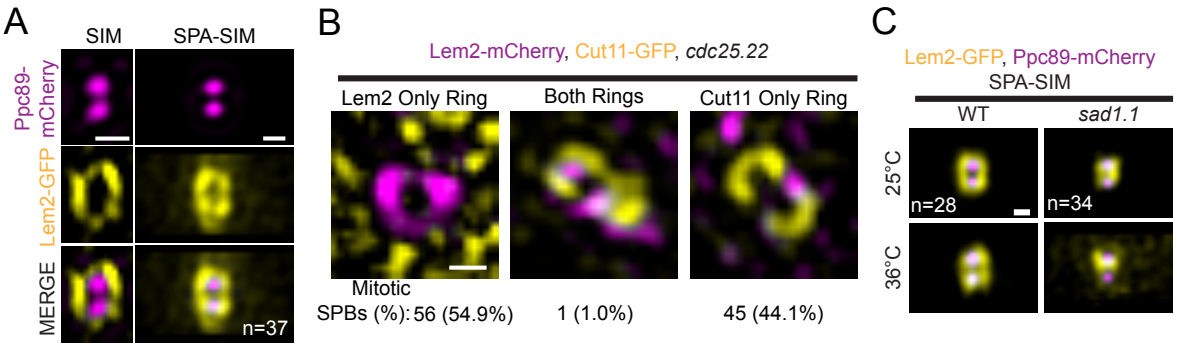

Figure S2. Lem2 forms a unique ring during interphase and early mitosis. (A) *cdc25.22* arrested cells containing Lem2-GFP (yellow) and Ppc89-mCherry (magenta) were images by SIM. Individual SIM image (left) and SPA-SIM (right) from the indicated number of images. Bar, 200 nm. (B) Similarly, *cdc25.22* arrested cells containing Lem2-mCherry (magenta) and Cut11-GFP (yellow) were imaged by SIM. Three configurations were observed in the indicated fraction of cells: Lem2 ring with no Cut11 ring (left), Cut11 ring with no Lem2 ring (center), and rings of both Cut11 and Lem2 (right). n=102. Bar, 200 nm. (C) SPA-SIM images for Lem2-GFP in WT and *sad1.1* backgrounds grown at 25°C or 36°C for 4 h. n, number of individual SIM images utilized for averaging. Bar, 200 nm.

Bqt4 (Hirano et al., 2018; Hu C et al., 2019); Cmp7 (Gu et al., 2017) and Ima1 (Hiraoka et al., 2011; Steglich et al., 2012). The only single gene deletion mutant to significantly affect Sad1 ring formation was *csi1Δ*, where we observed a 29.6% reduction in ring formation at 36°C (Fig 3D-E, Fig S1C). Although *lem2Δ* did not have a phenotype on its own (Fig S1C), its loss further exacerbated *csi1Δ* resulting in a 36.1% decrease in Sad1-GFP ring formation in *lem2Δ csi1Δ* at 36°C as well as a defect at 25°C (Fig 3D-E). Thus, Csi1 and to a lesser degree Lem2 play a role in Sad1 ring formation.

Attachment to the centromere is essential to Sad1 SPB ring formation

Previous work showed that *sad1.2* mutants are partially defective in centromere-binding (Fernandez-Alvarez et al., 2016). To test if centromeres are directly involved in Sad1 reorganization at mitosis, we first examined the ability of *sad1.2-GFP* to form SPB rings (Fig 4A). At 25°C, 95.5% of cells contain a sad1.2-GFP ring. This decreases to 78.9% if cells are shifted to 36°C for 4 h and further decreases to 36.5% after 8 h at 36°C (Fig 4B). If we combined *sad1.2* with *csi1Δ*, only 80.8% of cells contained a sad1.2-GFP ring at 25°C. A more pronounced, but not significant, defect was observed at 36°C where 66.0% or 22.7% of cells contained a sad1.2-GFP ring after 4 or 8 h, respectively (Fig 4A-B). The observation that *csi1*Δ did not exacerbate sad1.2-GFP ring formation at 36°C indicates that centromeric attachment is largely abolished due to the mutation in *sad1+*. The finding that the *csi1*Δ *sad1.2* double mutant showed reduced ring formation at 25°C suggests that while Csi1 is a major linker for Sad1 and the centromere, it is not the only attachment factor. This is consistent with our and others' data that *csi1*Δ is only partially penetrant (Hou et al., 2012; Fernandez-Alvarez and Cooper, 2017).

Figure 4

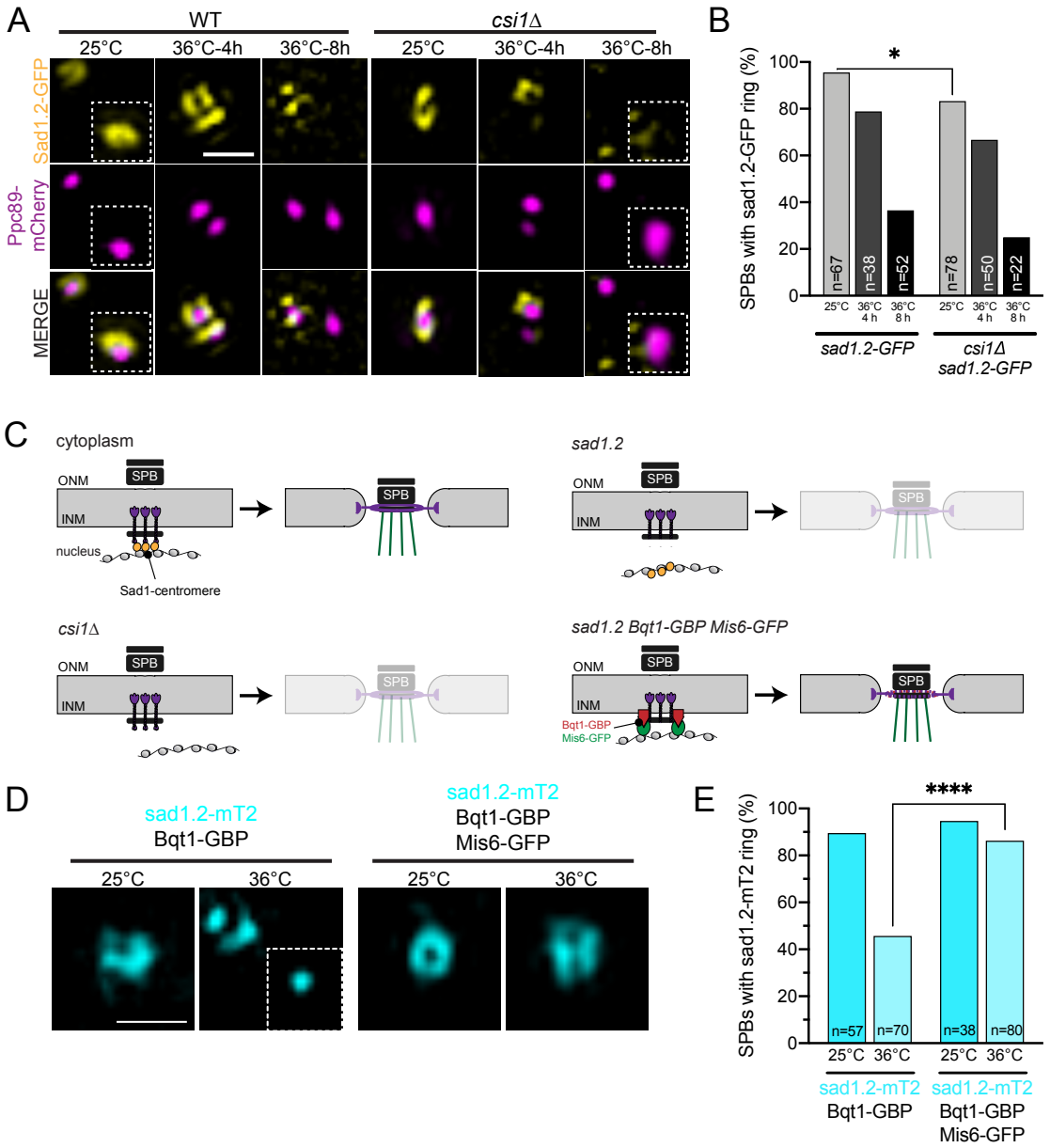

Figure 4. Sad1 attachment to the centromere is vital for Sad1 mitotic ring formation. (A-B) sad1.2-GFP (yellow) in wild-type or *csi1*Δ cells with Ppc89-mCherry (magenta) were grown at 25°C for 4 h or at 36°C for 4 and 8 h before imaging. (A) Representative SIM images of sad1.2-GFP rings at the SPB. The second SPB is shown in the inset. (B) Percentage of mitotic SPBs with a sad1.2-GFP ring. P values were determined using the χ^2 test. All are not significant, except *, p=0.007. (C) Schematic of centromere binding to the SPB. In wild-type cells (upper left), Sad1 (purple) is tethered by Csi1 (yellow) to the centromere, which leads to Sad1 ring formation at mitotic entry. Defects in the centromere attachment through *csi1Δ* (lower left) or *sad1.2* (upper right) disrupted Sad1 ring formation. To test if centromere attachment is sufficient to form the

Sad1 ring, an artificial tethering system using Bqt1-GBP (lower right), which binds to both sad1.2 and Mis6-GFP was used. (D-E) sad1.2-mT2 Bqt1-GBP with and without Mis6-GFP were grown at 25°C for 4 h or at 36°C for 8 h. (D) Representative SIM images of sad1.2-mT2 (cyan) mitotic rings. (E) Percentage of cells with sad1.2-mT2 rings. P values were determined using the χ^2 test. All are not significant, except ****, $p<0.001$. Bars, 500 nm.

To confirm that centromere attachment alone was required for Sad1 reorganization, we rescued the *sad1.2* SPB ring formation defect by forcing centromere-SPB attachment using a previously described GFP-binding protein (GBP) fused to Bqt1, a meiotic protein that is still able to bind to the N-terminus of sad1.2 (Fernandez-Alvarez et al., 2016). By adding GFP to a centromeric protein, Mis6 (Mis6-GFP), we can trigger centromere tethering: Mis6-GFP binds Bqt1-GBP, which then binds to sad1.2 (Fig 4C). In the Bqt1-GBP background, sad1.2-mTurquoise2 (mT2) SPB ring formation drops from 89.5% at 25°C to 45.7% at 36°C for 8 h, similar to sad1.2-GFP levels seen above. However, when we force centromere attachment with Mis6-GFP in the Bqt1-GBP background, then sad1.2-mT2 ring formation is fully rescued (Fig 4D-E). Collectively, these experiments show that centromere attachment alone is sufficient to drive Sad1 ring formation in mitotic cells. While the centromeric DNA itself could lead to remodeling, we hypothesized that a signaling molecule associated with the centromeres drives Sad1 reorganization. Using Sad1 distribution, we assayed factors involved centromere-based signaling coincident with mitotic entry to test this idea.

Complete SPB ring formation and NEBD is regulated by Polo Kinase

Entry into mitosis is exquisitely regulated in most organisms to ensure that NEBD, spindle formation and chromosome segregation only occur once DNA replication has been completed. In fission yeast, a network of kinases and phosphatases control the G2/M transition (reviewed in Hagan IM, 2008), including the highly conserved cyclin-dependent kinase (CDK), *cdc2*+ (Nurse and Thuriaux, 1980); Polo kinase, *plo1*+

(Ohkura, Hagan and Glover, 1995); and Aurora B kinase, *ark1+* (Petersen et al., 2001; Leverson et al., 2002).

To inactivate *ark1+* and *plo1+*, we utilized temperature-sensitive strains, *ark1-T7* (Bohnert et al., 2009) and *plo1-24c* (Bähler et al., 1998), while for *cdc2+*, we utilized an analog-sensitive strain, *cdc2-asM17* (Aoi et al., 2014). Each of these kinase mutants were put into restrictive conditions for 4 h and then assayed for Sad1 ring formation (Fig 5A). *cdc2-asM17* had no effect on Sad1 ring formation as 96.4% of cells at the non-permissive condition formed Sad1 rings, which is very similar to wild-type levels (97.6%). *ark1-T7* mutants displayed a mild (83.8%) decrease in Sad1 ring formation at 36°C, but the most significant loss was seen with *plo1-24c*, which had only 38.5% Sad1 ring formation at 36°C (Fig 5A-B). This suggests that Polo kinase is required at some step of Sad1 reorganization.

One particularly tempting idea is that the centromere delivers Polo to the SPB to initiate Sad1 reorganization and NEBD. This model leads to several testable predictions: Plo1 should localize to the nuclear face of the SPB near Sad1 and the centromere, and Polo kinase function should be required for initiation of Sad1 reorganization as well as for all downstream steps, including Cut12 recruitment and NEBD. Plo1 has multiple targets that localize throughout the cell, but the kinase is known to localize to the SPB during mitosis (Mulvihill et al., 1999). High resolution SPA-SIM analysis of Plo1-GFP distribution showed that at the G2/M boundary, the majority of Polo kinase at the SPB is present at the bridge region, which connects the duplicated SPBs marked by Ppc89-

Figure 5

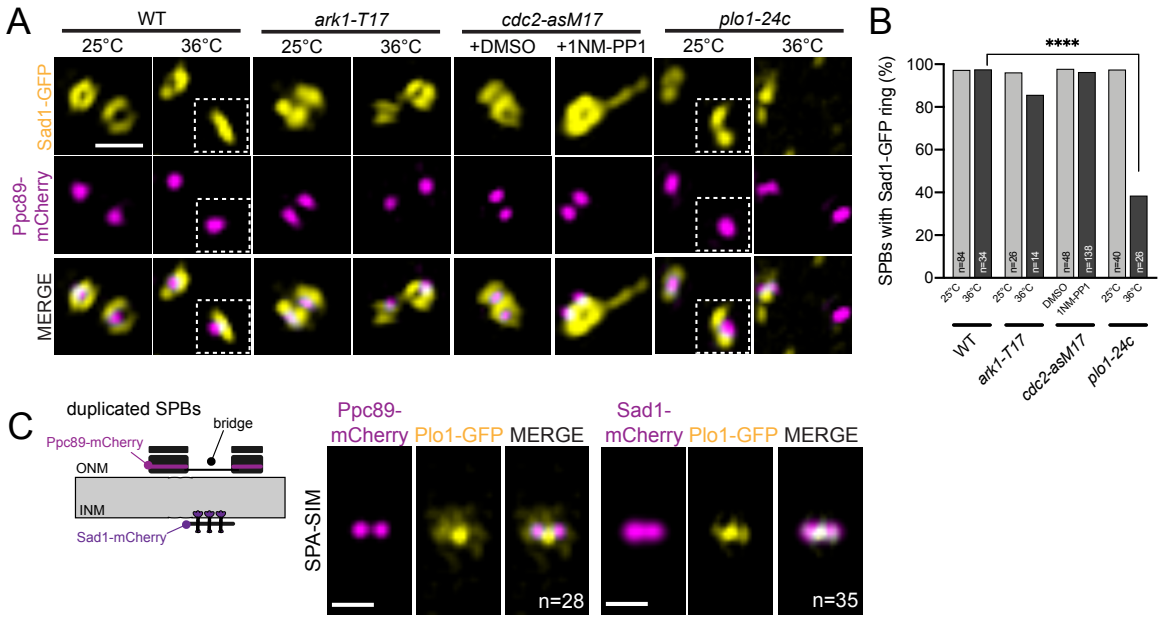

Figure 5. Polo kinase is necessary for Sad1 ring formation. (A-B) Sad1-GFP (yellow) and Ppc89-mCherry (magenta) in mitotic kinase mutants (from left to right): wild-type; Aurora B kinase (*ark1-T17*); Cdk1 (*cdc2-asM17*) and Polo kinase (*plo1-24c*). Cells were grown at 25°C or at 36°C for 4 h (WT, *ark1-T17, plo1-24c)* or in the presence of 50 µM DMSO or 1NM-PP1 for 4 h before imaging. (A) Representative SIM Images of early mitotic cells. Inset shows second SPB. (B) Percentage of mitotic cells with a Sad1 ring at the SPB. P values compared to wild-type were determined using the χ^2 test. All are not significant, except ****, $p<0.001$. (C) Schematic showing duplicated side-by-side SPBs connected by a bridge on the cytoplasmic face of the ONM. Ppc89 localizes to each SPB core, while Sad1 is present at the INM (Bestul et al. 2017). SPA-SIM of Plo1-GFP (yellow) with Ppc89-mCherry or Sad1-mCherry (magenta) in cells at G2/M using *cdc25.22*. n, number of individual SIM images utilized for averaging. Bars, 500 nm.

mCherry (Fig 5C). The co-localization of Plo1-GFP and Sad1-mCherry along with the offset from Ppc89-mCherry indicates that Plo1 is recruited at the INM face of the SPB upon mitotic entry (Fig 5C). This unexpected localization puts the bulk of Plo1 at the same spot as the centromere (Fig S1B) and in a location to interact with Sad1.

We were interested in testing if Polo kinase had an early mitotic function that would correspond to the localization to the INM face of the SPB we observed. To test if loss of *plo1+* function specifically affects mitotic entry, we utilized a *plo1+* analog-sensitive strain, *plo1.as8* (Grallert et al., 2013a), in a *cdc25.22* background. Cells were arrested at G2/M by growth at 36°C for 3 h, then the *plo1.as8* inhibitor (3Brb-PP1) was added to inactivate Polo kinase for another 30 min while cells were kept at 36°C. Cultures were then released from G2/M by shifting cells to 25°C in the presence of 3Brb-PP1 to study Sad1 ring formation, Cut12 recruitment and NEBD in the absence of Polo kinase (Fig 6A).

Compared to controls in which virtually all (99%) cells contained at Sad1-GFP ring, 75.6% of cells in which *plo1.as8* was inhibited reorganized Sad1-GFP (Fig 6B-C). Analysis of the rings in control and *plo1.as8* inhibited cells showed a defect in ring maturation in the absence of Polo kinase: only 36% of the rings in *plo1.as8* inhibited cells were mature double rings compared to 95-97% of controls (Fig 6C). This data implies that Polo kinase plays a vital role in Sad1 ring maturation, however, its function is likely not required or is redundant with other factors for initiation of Sad1 redistribution.

To further define the events downstream of Sad1 ring initiation that might require Polo, we examined Cut12-GFP, which showed a significant reduction in recruitment to rings when Polo kinase activity was inhibited (from 91.9% to 31.7% for Cut12-GFP in *cdc25.22 plo1.as1* cells without and with 3Bbr-PP1) (Fig 6B & D). Thus, Polo acts upstream of Cut12 but downstream of Sad1. Consistent with this idea, we found that *cdc25.22 plo1.as8* cells did not lose NE integrity, as the strain with the inhibitor had the same N:C ratio of GFP fluorescence (2.8±0.1) as without the inhibitor (2.8±0.1) (Fig 6E). Taken together, our data supports a new nuclear role for Polo kinase to regulate Sad1 ring maturation and initial NEBD at mitotic entry.

To confirm that centromere-mediated delivery of Polo kinase to the SPB is needed for Sad1 ring maturation, we triggered sad1.2-mT2 redistribution with forced centromere binding (Bqt1-GBP, Mis6-GFP) while at the same time inhibiting *plo1.as8* with 3Brb-PP1 Without the analog or in controls, centromere attachment resulted in sad1.2-mT2 ring formation in ~80% of cells (Fig 4C-E; 6F-G). However, the fraction of *plo1.as8* strains with sad1.2-mT2 rings dropped to 46.6% in the presence of the inhibitor (Fig 6G). Examination of individual SPBs showed a full or partial sad1.2-mT2 ring around one of the two SPBs in the absence of Polo activity, but at the second SPB, ring formation did not occur (Fig 6F). Thus, the centromere itself is insufficient without Polo, which is needed to complete ring formation around both SPBs.

Figure 6

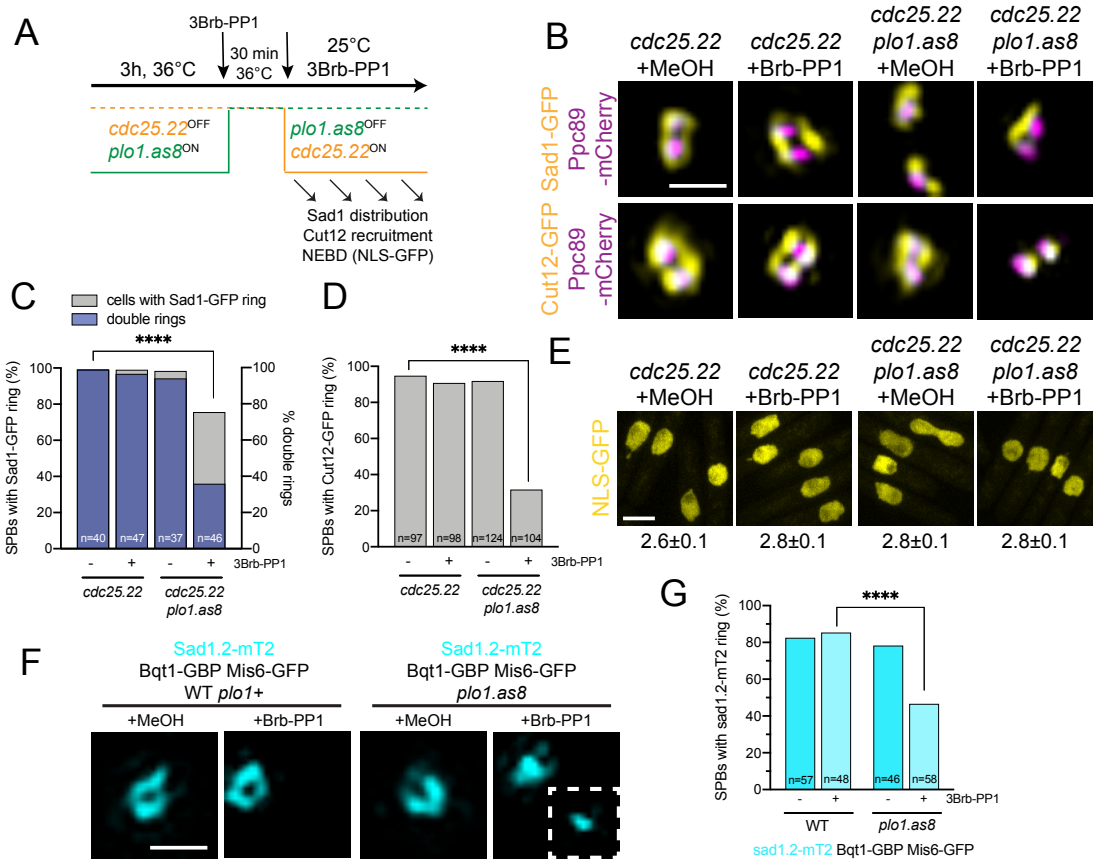

Figure 6. Polo kinase is required for NEBD. (A) To examine if Polo is required at mitotic entry for ring formation, *cdc25.22 plo1.as8* cells were grown for 3 h at 36°C to inactivate *cdc25.22*. Then 3Brb-PP1 was added for 30 min at 36°C to inactivate *plo1.as8*. Shifting cells to 25°C with 3Brb-PP1 for 30 min reactivates *cdc25.22* and allows cells to enter mitosis with inactive *plo1.as8*. (B-D) *cdc25.22* or *cdc25.22 plo1.as8* cells with Ppc89-mCherry (magenta) and Sad1-GFP or Cut12-GFP (yellow) were cultured as in Fig 6A. (B) Representative SIM images. Bar, 500 nm. (C) Percentage of mitotic SPBs that had any Sad1-GFP ring (gray) or a double Sad1-GFP ring (blue). (D) Percentage of mitotic SPBs that had any Cut12-GFP ring. P values for C-D compared to wild-type were determined using the χ^2 test. All are not significant, except ****, $p<0.001$. (E) Nuclear localization of 3nmt-NLS-GFP was assayed in *cdc25.22* or *cdc25.22 plo1-as8* to test for NEBD. Cells were grown as in Fig 6A before confocal imaging. Bar, 5 µm. The average ratio of total nuclear to cytoplasmic GFP fluorescence is listed below each image. Error, SEM. n=100. Based on individual t-tests, all differences are not statistically significant. (F-G) sad1.2-mT2 (cyan) in Bqt1-GBP/Mis6-GFP with wild-type *plo1+* or *plo1.as8* was tested for its ability to form rings by growing cells at 36°C for 8 h in the presence of 50 µM MeOH or 3Brb-PP1 before imaging. (F) Representative SIM image. A second SPB is shown in the inset. Bar, 500 nm. (G) Percentage of cells with sad1.2-mT2 rings. P values compared to wild-type were determined using the χ^2 test. All are not significant, except ****, $p<0.001$.

Discussion

SPB ring formation at early mitosis facilitates localized NEBD and mitotic progression with Sad1 as the gatekeeper

Utilization of super-resolution microscopy allowed us to visualize a novel mitotic SPB ring surrounding the *S. pombe* SPB for the first time. It contains the NE proteins Sad1 and Kms2, the mitotic regulatory protein Cut12 and the SPB insertion protein Cut11. While a toroidal structure around the SPB has been seen before in *S. cerevisiae* (Chen et al., 2019), the *S. pombe* ring is unique is three ways: 1) it only forms at mitotic entry and dissipates upon mitotic exit; 2) its formation is triggered by the centromere; and 3) Sad1 plays an essential role in ring assembly compared to the important, but non-essential, role of Mps3 in *S. cerevisiae* (Chen et al., 2019). The *S. cerevisiae* SPB is inserted into the NE during G1 phase with the help of local NPCs (Rüthnick et al., 2017), which are not observed adjacent to *S. pombe* SPBs (Ding et al., 1997; Uzawa et al., 2004; Tamm et al., 2011). The key role of the LINC complex (Sad1-Kms2/Kms1) in creating the SPB ring could explain how *S. pombe* might coordinate nuclear and cytoplasmic triggers for NE remodeling without NPCs. Importantly, this function of the LINC complex in regulated NEBD could possibly be utilized by other organisms that partially or completely dismantle the NE during mitosis.

Based on our data, we propose the following stepwise model of *S. pombe* ring assembly and NEBD upon mitotic entry (Fig 7). Duplicated SPBs sit on top of the intact NE prior to mitosis surrounded by a large ring of Lem2. During this stage, Sad1 is not

Figure 7

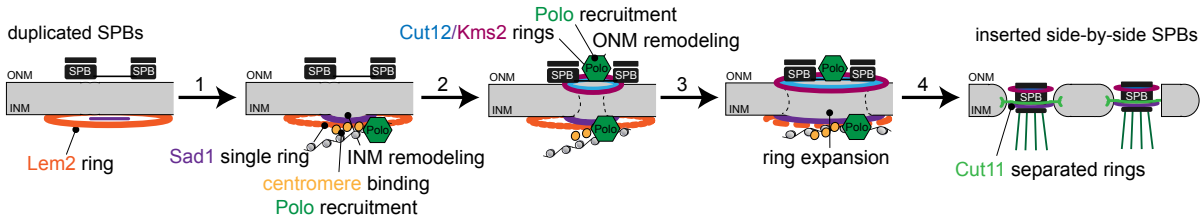

Figure 7. Model of mitotic SPB ring formation and NEBD at *S. pombe* mitotic entry. Duplicated SPBs sit on top of the nuclear envelope with no proteins in a ring structure except Lem2 prior to mitosis. (1) A centromere signal, helped by Csi1, leads to the “old” Sad1 reorganizing into a single ring, opening the INM, while also recruiting Polo. (2) Recruitment of cytoplasmic Polo, Cut12 and Kms2 opens the ONM, completing NEBD. (3) Polo both in the nucleus (modifying the “new” Sad1) and cytoplasm trigger SPB ring expansion to the double ring and encapsulates both SPBs. (4) As Lem2 dissipates, Cut11 is recruited to the mitotic SPBs, allowing SPB insertion and separation.

present in a ring but rather sits at the INM. (1) Upon mitotic entry, Sad1 is redistributed into a ring structure at the INM, mediated in part by centromere interactions. Polo is recruited to the nuclear face of the SPB. (2) Further recruitment of Polo kinase leads to redistribution of Kms2 and Cut12. NEBD beneath the SPB is completed. (3) Continued recruitment of Polo kinase via Kms2 to the ONM and via the centromere at the INM results in ring expansion. (4) Lastly, Cut11 is recruited and Lem2 disappears from the SPB ring. This enables the nascent SPBs to insert into the SPB fenestrae and 'plug the hole' to prevent complete NEBD. This timeline provides a snapshot of events leading to NEBD, and it provides a framework from which we can begin to study NEBD at a mechanistic level to address gaps in our model. For example, how is Polo kinase recruited by the centromere? How do Sad1, Kms2 and Cut12 drive NE remodeling? How do Cut11 and Lem2 drive SPB separation?

The role of the centromere and centromeric proteins in regulating ring formation

Linkage of chromosomes, specifically telomeres, to the SPB is vital for fission yeast meiosis (Tomita and Cooper, 2007; Klutstein and Cooper, 2014). Although centromeres can substitute for telomeres in meiosis, typically centromere-SPB attachment occurs during mitosis (Fernandez-Alvarez et al., 2016). Here, we show that this connection is needed for SPB ring formation downstream of Sad1 and for NEBD/SPB insertion. Csi1 and Lem2 were tested for their ability to serve as linker proteins between the centromere and Sad1. Although both proteins formed ring-like structures around the SPB, the size and timing of Csi1 rings made it a leading candidate as a Sad1 regulator. Consistent with this idea, Csi1 is known to bind Sad1 and the outer kinetochore protein

Spc7 (Hou et al., 2012). Loss of Csi1 function disrupts centromere clustering underneath the SPB (Hou et al., 2012), and Csi1 deletion, when combined with the *sad1.2* mutation causes severe loss of Sad1 ring formation (Fig 4A, B). However, residual Sad1 ring formation in this mutant suggests redundant mechanisms for centromere tethering, possibly through other Sad1-centromere interacting factors or centromere-independent Sad1 regulation.

Lem2 also interacts with Sad1 and the centromere (Hiraoka et al., 2011). Our observation the Lem2 is distributed in a large ring surrounding the SPB during interphase and that its localization to this region dissipates early in mitosis suggests that it only indirectly affects the mitotic SPB, as the *lem2Δ* strain did not affect Sad1 ring formation (Fig S1B). Interestingly, the Lem2 SPB rings completely disappear just before SPB separation at the time when Cut11 localizes to the SPB (Fig S2B). One possibility is that Cut11 replaces Lem2 to drive SPB separation.

Depletion of CENP-A was recently shown to disrupt mitotic spindle formation and displace centrioles (Gemble et al., 2019), a phenotype that is reminiscent of the spindle assembly and disconnected SPBs seen in the *sad1.2* mutant in *S. pombe* (Fernandez-Alvarez et al., 2016). Thus, a key question is how the centromere, centrosome/SPB and spindle coordinate activity to ensure the integrity of the mitotic spindle. We hypothesized that centromeric attachment to the SPB via Sad1 delivered a mitotic regulator to instigate Sad1 reorganization and facilitate NEBD. Using Sad1 ring formation as an

assay, we were able to test key mitotic kinases and uncover an unexpected role for Polo kinase.

Regulation of NEBD through mitotic kinases

In fission yeast, Plo1 is perhaps best known for its role in mitotic activation feedback. Previous work showed that Polo kinase interacts with the SPB components Cut12 and Kms2 to promote mitotic cyclin-Cdk inactivation through the Cdc25 phosphatase and the Wee1 kinase (Walde and King, 2014; Gallert et al., 2013; MacIver et al., 2003). Our data suggest an additional role for Polo kinase, which is likely delivered to the nuclear face of the SPB by the centromere. Interestingly, Sad1 ring formation at one SPB is unaffected by loss of Plo1 while ring formation at the second SPB is blocked (Fig 6F, G). We propose that Plo1 is needed to phosphorylate newly recruited Sad1 at the 'new' SPB, licensing the pole for NE insertion, while the 'old' Sad1 was licensed by Plo1 from the previous cell cycle. However, as we have yet to detect direct Plo1 phosphorylation of Sad1, other intermediates may be involved.

Differences in the 'old' and 'new' SPB have been previously reported in *cut12.1*, *81nmt1-GFP-Kms2*, *cut11.1* and *sad1.2* mutants: in each case, the 'old' SPB is competent to insert into the NE while the 'new' SPB exhibits insertion defects. In many cases this is accompanied with a loss of NE integrity and loss of a soluble GFP reporter. Our data brings a new understanding to these phenotypes in several ways. First, the SPB insertion failure is the result of defects in initiation/progression of the mitotic ring

cascade. Second, because breakdown of the NE is triggered early in the pathway, mutants defective in SPB insertion will have a loss of NE integrity.

Polo kinase in *S. pombe* interacts with Cut12 and Kms2 extensively. Our SIM data showing the bulk of Polo at the INM surface of the SPB at the G2/M transition is not inconsistent with these data as our results come from arrested cells and would be unable to account for the entire population of Plo1. Perhaps the most intriguing question is how Plo1 binds to the SPB throughout insertion. Does it first bind to Sad1 in the nucleus, then interact with Cut12 and Kms2 in the cytoplasm after mitosis is initiated? Or does Plo1 bound to Sad1 get 'delivered' to Cut12 and Kms2 via NE remodeling? Somewhat surprisingly, Sad1 ring formation was not dependent on Cdk activity despite having two residues targeted by the kinase (Swaffer MP et al., 2018). The loss of *cdc2*+ created more robust Sad1 SPB rings, with significant Sad1 localization away from the SPB (Fig 5A). This suggests mitotic Cdk activity may regulate Sad1 levels in mitotic cells to prevent the formation of ectopic sites of NEBD.

In conclusion, our observations bring to light that redistribution of SPB, NE and centromere proteins in a coordinated fashion is vital to NEBD and mitotic progression. In fission yeast, this process is not regulated by mitotic Cdk but instead it is regulated almost exclusively by the Polo kinase, Plo1. Polo-like kinases facilitate NEBD in *C. elegans* (Rahman et al., 2015) and humans (Lenart et al., 2007), raising the interesting possibility that centromere-linkage, protein redistribution and Polo kinase regulation is more generally involved in nuclear remodeling.

Materials and Methods

Yeast Strains and strain construction

S. pombe strains used in this study are listed in Table S1, including strains we received from other laboratories: *sad1.2-GFP-KanMX6* and *sad1.2:NatMX6, bleMX6-nmt3X-bqt1-GBP-mCherry:HygMX6, Pnda3-mCherry-atb2:aur1R, Mis6-GFP:kanMX6* (J.P. Cooper, University of Colorado, Denver, CO); *ark1-T7* and *plo1-24c* (K.L. Gould, Vanderbilt University, Nashville, TN); *cdc2-asM17* (K.E. Sawin, University of Edinburgh, Edinburgh, UK); *plo1-GFP-KanMX6* (A. Paoletti, PSL Research University, Paris, France); *plo1.as8-Ura4+* (I.M. Hagan, University of Manchester, Manchester, UK). All fusions to GFP and/or mCherry not listed above were created using PCR-based methods that targeted the endogenous locus as described (Bahler et al., 1998). Additional strains were made through standard genetic crosses.

Cell cycle growth and fixation

To analyze SPB protein distribution at mitotic entry, *cdc25.22* strains with fluorescently tagged SPB components were grown in yeast-extract (YE5S) media for ~40 h at 25°C, with back dilutions to ensure cells remained logarithmic. Then strains were diluted into Edinburgh minimal media with amino acid supplements (EMM5S) and allowed to grow for 2 h at 25°C before being transferred to 36°C for 3.5 h. Cells were either collected at this time for fixation (see below) or transferred to 25°C for 10, 20 and 30 min before fixation.

To study *sad1.1*, *cut11.1*, or *cut12.1*, strains were also grown in YE5S media for ~40 h at 25°C, diluted into EMM5S for 2 h at 25°C, transferred to 36°C for 4 h and then collected for fixation. If strains contained a construct expressed from the *nmt1* promoter (*nmt1-3x-NLS-GFP* and *41nmt1-GFP-Kms2*), growth times and media were altered. Strains were first streaked to EMM5S plates for at least 2 d, then grown in EMM5S media for ~24 h at 25°C, with back dilutions to ensure cells remained logarithmic. After the 24 h, strains were treated as above for growth and fixation.

To analyze loss of *kms2*+ function, *81nmt1-HA-Kms2* strains were streaked out to EMM5S plates for at least 2 d, and then grown in EMM5S media for ~24 h at 25°C, with back dilutions to ensure cells remained logarithmic. Then 10 μM of thiamine was added to the EMM5S to shut off *kms2*+ expression for ~16 h at 25°C, and then cells were fixed.

Analog-sensitive alleles of Polo (*plo1-as8*) and Cdk (*cdc2-asM17*) were inactivated as follows. Cells were grown in YE5S media for ~40 h at 25°C, with back dilutions to ensure cells remained logarithmic. After diluting into EMM5S for 2 h at 25°C, 50 μM of 1NM-PP1 (Sigma-Aldrich; dissolved in DMSO, *cdc2-asM17*) or 3Brb-PP1 (AbCam; dissolved in methanol, *plo1-as8*) or the vehicle only were added. Cells were then grown for 2 or 4 h before fixation. After 2 h at 25°C in EMM5S, *cdc25.22 plo1-as8* were transferred to 36°C for 3 h before addition of 50 μM 3Brb-PP1/methanol, after which they were allowed to incubated at 36°C for an additional 30 min. Cells were then released from *cdc25.22* by growth at 25°C for 30 min before fixation.

Cells were fixed with 4% paraformaldehyde (Ted Pella) in 100 mM sucrose for 20 min, pelleted by brief centrifugation and then washed twice in PBS, pH 7.4. After the last wash, excess PBS was removed and ~20 µl of PBS was left to resuspend the cells for visualization by SIM. Fixed cells were kept at 4°C for up to 7 d before imaging.

SIM imaging and SPA-SIM

SIM imaging utilized an Applied Precision OMX Blaze V4 (GE Healthcare) using a 60x 1.42 NA Olympus Plan Apo oil objective and two PCO Edge sCMOS cameras (one camera for each channel). All SIM microscopy was performed at room temperature (22°C-23°C). For the two-color GFP/mCherry experiments, a 405/488/561/640 dichroic was used with 504- to 552-nm and 590- to 628-nm emission filters for GFP and mCherry, respectively. Images were taken using a 488-nm laser (for GFP) or a 561-nm laser (for mCherry), with alternating excitation. SIM reconstruction was done with Softworx (Applied Precision Ltd.) with a Wiener filter of 0.001. SIM images shown in the publication are maximum projections of all z-slices, scaled 8 x 8 with bilinear interpolation using ImageJ (National Institutes of Health) to enlarge the images.

SPA-SIM analysis was performed with custom written macros and plugins in ImageJ. All plugins and source code are available at http://research.stowers.org/imagejplugins/. Individual spots of mother and satellite SPBs were fitted to two 3D Gaussian functions and realigned along the axis between these functions for further analysis using [jay_sim_fitting_macro_multicolor_profile_NPC.ijm]. Spot selection was performed in a

semiautomated fashion with manual identification and selection of mother and satellite SPBs. A secondary protein (Ppc89-mCherry) was used as a fiduciary marker to determine position of the GFP-labeled protein so that all positions of the SPB proteins were compared with a single origin point. For the fiducial protein, the higher intensity spot was assigned as the mother. After alignment, images were averaged and scaled as described previously (Burns et al., 2015), using [merge_all_stacks_jru_v1.ijm] then [stack_statistics_jru_v2.ijm].

To quantitate the distribution of GFP-tagged SPB proteins and assess ring formation, images containing the GFP-tagged protein and Ppc89-mCherry were used. Individual images were manually inspected and analyzed. If the GFP signal encompassed over 50% of the Ppc89-mCherry signal, it was counted as a ring. In some cases, the ring was in the z-axis (thus not visible as a ring in the xy-plane); if the GFP signal extended beyond the Ppc89-mCherry signal for more than 50 nm in both directions, then it was also tabulated as a ring. Because of the small size of some rings and the limited resolution of SIM (particularly in the z-axis), not all rings had a distinct center.

Confocal imaging and analysis

Confocal imaging utilized a PerkinElmer UltraVIEW VoX with a Yokogawa CSU-X1 spinning disk head, a 100x 1.46 NA Olympus Plan Apo oil objective and CCD (ORCA-R2) and EMCCD (C9100-13) cameras. All confocal microscopy was performed at room temperature (22°C-23°C). For the two-color GFP/mCherry experiments, images were

taken using a 488-nm laser (for GFP) or a 561-nm laser (for mCherry), with alternating excitation. Images were collected using the Volocity imaging software.

To quantify how the various SPB mutants affected GFP-tagged localization, 5 μm z-stack images were taken with above equipment, with a step size of 0.3 μm per slice (17 slices total). The entire z-stack was sum projected using ImageJ, and the Ppc89-mCherry was used as the SPB marker to tally the number of mCherry puncta (Ppc89) that also had GFP puncta (Sad1, Cut12, Kms2 and Cut11) present or absent.

To measure the intensity of NLS-GFP, sum projections of the entire z-stack were created using ImageJ. After background subtraction, a region of interest (ROI) was drawn around each nucleus and the integrated fluorescence intensity was divided by the area of the ROI. This ROI was then used to measure the integrated fluorescence intensity of the cytoplasm of that cell. The integrated fluorescence intensity of the nucleus over the cytoplasm gave a N:C ratio for each cell. The average of this ratio for 100 cells was determined.

Supplementary information

Figure S1. Sad1 ring formation is co-incident with the centromere.

Figure S2. Lem2 forms a unique ring during interphase and early mitosis.

Table S1. Yeast Strains.

Acknowledgements

We are grateful to Julie Cooper, Kathy Gould, Ken Sawin, Anne Paoletti and Iain Hagan for reagents and to the Jaspersen Lab for discussions and comments on the manuscript. Research reported in this publication was supported by the Stowers Institute for Medical Research and the NIH-NIGMS under award number R01GM121443 (to SLJ). Original data underlying this manuscript can be downloaded from the Stowers Original Data Repository at http://www.stowers.org/research/publications/LIBPB-xxxx. The authors declare no competing financial interests.

Author Contributions

AJB and SLJ conceived the experiments, AJB constructed strains and performed experiments, ZU assisted with SIM, JRU developed tools for image analysis, AJB prepared figures, and AJB and SLJ wrote the paper with input from all the authors.

Abbreviations

MTOC, microtubule-organizing center; SPB, spindle pole body; SIM, structured illumination microscopy; EM, electron microscopy; NE, nuclear envelope; NPC, nuclear pore complex; SPA, single particle analysis; SEM, standard error of the mean; EM, electron microscopy; SPIN, spindle pole body insertion network; SUN, Sad1-UNC-84 homology; KASH, Klarisht-ANC-1-Syne-1 homology; LINC, linker of nucleoskeleton and cytoskeleton; mT2, mTurquoise2; NEBD, nuclear envelope break down; CDK, cyclin-dependent kinase; ROI, region of interest

References

Aoi Y., S.A. Kawashima, V. Simanis, M. Yamamoto and M. Sato, Optimization of the analogue-sensitive Cdc2/Cdk1 mutant by in vivo selection eliminates physiological limitations to its use in cell cycle analysis. *Open Biol.* 2014 Jul; 4(7): 140063. Doi: 10.1098/rsob.140063.

Asakawa H., A. Hayashi, T. Haraguchi and Y. Hiraoka. Dissociation of the Nuf2-Ndc80 complex releases centromeres from the spindle-pole body during meiotic prophase in fission yeast. *Mol Biol Cell*. 2005 May; 16(5):2325-38. Doi: 10.1091/mbc.e04-11-0996.

Bähler J., J.Q. Wu, M.S. Longtine, N.G. Shah, A. McKenzie 3rd, A.B. Steever, A. Wach, P. Philippsen and J.R. Pringle. Heterologous modules for efficient and versatile PCR-based gene targeting in Schizosaccharomyces Pombe. *Yeast*. 1998 Jul; 14(10):943-51. Doi: 10.1002/(SICI)1097-0061(199807)14:10<943::AID-YEA292>3.0.CO;2-Y.

Banday S., Z. Farooq, R. Rashid, E. Abdullah and M. Altaf. Role of inner nuclear membrane protein complex Lem2-Nur1 in heterochromatic gene silencing. *J Biol Chem*. 2016 Sep 16; 291(38):20021-9. Doi: 10.1074/jbc.M116.743211.

Barrales R.R., M. Forn, P.R. Georgescu, Z. Sarkadi and S. Braun. Control of heterochromatin localization and silencing by the nuclear membrane protein Lem2. *Genes Dev*. 2016 Jan 15; 30(2):133-48. Doi: 10.1101/gad.271288.115.

Bestul A.J., Z. Yu, J.R. Unruh and S.L. Jaspersen. Molecular model of fission yeast centrosome assembly determined by superresolution imaging. *J Cell Biol.* 2017 Aug 7; 216(8):2409-2424. Doi: 10.1083/jcb.201701041.

Bettencourt-Dias M. and D.M. Glover. Centrosome biogenesis and function: centrosomics brings new understanding. *Nat Rev Mol Cell Biol.* 2007 Jun; 8(6):451-63. Doi: 10.1038/nrm2180.

Bohnert K.A., J.S. Chen, D.M. Clifford, C.W. Vander Kooi and K.L. Gould. A link between aurora kinase and Clp1/Cdc14 regulation uncovered by the identification of a fission yeast borealin-like protein. *Mol Biol Cell.* 2009 Aug; 20(16):3646-59. Doi: 10.1091/mbc.e09-04-0289.

Burns S., J.S. Avena, J.R. Unruh, Z. Yu, S.E. Smith, B.D. Slaughter, M. Winey and S.L. Jaspersen. Structured illumination with particle averaging reveals novel roles for yeast centrosome components during duplication. *Elife.* 2015 Sep 15; 4:e08586. Doi:10.7554/eLife.08586.

Cavanaugh A.M. and S.L. Jaspersen. Big Lessons from Little Yeast: Budding and Fission Yeast Centrosome Structure, Duplication and Function. *Annu Rev Genet*. 2017 Nov 27; 51:361-383. Doi: 10.1146/annurev-genet-120116-024733.

Chen J., J.M. Gardner, Z. Yu, S.E. Smith, S. McKinney, B.D. Slaughter, J.R. Unruh and S.L. Jaspersen. Yeast centrosome components form a noncanonical LINC complex at the nuclear envelope insertion site. *J Cell Biol.* 2019 Mar 12; 218(5):1478-1490. Doi: 10.1083/jcb.201809045.

Chikashige Y., C. Tsutsumi, M. Yamane, K. Okamasa, T. Haraguchi and Y. Hiraoka. Meiotic proteins Bqt1 and Bqt2 tether telomeres to form the bouquet arrangement of chromosomes. *Cell.* 2006 Apr 7; 125(1):59-69. Doi: 10.1016/j.cell.2006.01.048.

Decottignies A., P. Zarzov and P. Nurse. In vivo localization of fission yeast cyclin-dependent kinase Cdc2p and cyclin B Cdc13p during mitosis and meiosis. *J Cell Sci.* 2001 Jul; 114(Pt 14):2627-40. PMID: 11683390.

Ding R., R.R. West, D.M. Morphew, B.R. Oakley and J.R. McIntosh. The spindle pole body of Schizosaccharomyces Pombe enters and leaves the nuclear envelope as the cell cycle proceeds. *Mol Biol Cell.* 1997 Aug; 8(8):1461-79. Doi: 10.1091/mbc.8.8.1461.

Fennell A., A. Fernandez-Alvarez, K. Tomita and J.P. Cooper. Telomeres and centromeres have interchangeable roles in promoting meiotic spindle formation. *J Cell Biol.* 2015 Feb 16; 208(4):415-28. Doi: 10.1083/jcb.201409058.

Fernandez-Alvarez A., C. Bez, E.T. O'Toole, M. Morphew and J.P. Cooper. Mitotic nuclear envelope breakdown and spindle nucleation are controlled by interphase

contacts between centromeres and the nuclear envelope. *Dev Cell.* 2016 Dec 5; 39(5):544-559. Doi: 10.1016/j.devcell.2016.10.021.

Fernandez-Alvarez A. and J.P. Cooper. The functionally elusive Rabl chromosome configuration directly regulates nuclear membrane remodeling at mitotic onset. *Cell Cycle*. 2017 Aug 3; 16(15):1392-1396. Doi: 10.1080/15384101.2017.1338986.

Funabiki H., I.M. Hagan, S. Uzawa and M. Yanagida. Cell cycle-dependent specific positioning and clustering of centromeres and telomeres in fission yeast. *J Cell Biol*. 1993 Jun; 121(5):961-76. Doi: 10.1083/jcb.121.5.961.

Ganem N.J., S.A. Godinho and D. Pellman. A mechanism linking extra centrosomes to chromosomal instability. *Nature.* 2009 Jul 9; 460(7252):278-82. Doi: 10.1038/nature08136.

Gemble S., A. Simon, C. Pennetier, M. Dumont, S. Herve, F. Meitinger, K. Oegema, R. Rodriguez, G. Almouzni, D. Fachinetti and R. Basto. Centromere dysfunction compromises mitotic spindle pole integrity. *Curr Biol.* 2019 Sep 23; 29(18):3072-3080.e5. doi: 10.1076/j.cub.2019.07.052.

Gönczy P. Centrosomes and cancer: Revisiting a long-standing relationship. *Nat Rev Cancer.* 2015 Nov; 15(11):639-52. Doi: 10.1038/nrc3995.

Grallert A., A. Patel, V.A. Tallada, K.Y. Chan, S. Bagley, A. Krapp, V. Simanis and I.M. Hagan. Centrosomal MPF triggers the mitotic and morphogenetic switches of fission yeast. *Nat Cell Biol.* 2013 Jan; 15(1):88-95. Doi: 10.1038/ncb2633.

Grallert A., K.Y. Chan, M.L. Alonso-Nunez, M. Madrid, A. Biswas, I. Alvarez-Tabares, Y. Connolly, K. Tanaka, A. Robertson, J.M. Ortiz, D.L. Smith and I.M. Hagan. Removal of centrosomal PP1 by NIMA kinase unlocks the MPF feedback loop to promote mitotic commitment in S. pombe. *Curr Biol.* 2013 Feb 4; 23(3):213-22. Doi: 10.1016/j.cub.2012.12.039.

Gu M., D. LaJoie, O.S. Chen, A. von Appen, M.S. Ladinsky, M.J. Redd, L. Nikolova, P.J. Bjorkman, W.I. Sundquist, K.S. Ullman and A. Frost. Lem2 recruits Chmp7 for ESCRT-mediated nuclear envelope closure in fission yeast and human cells. *Proc Natl Acad Sci U S A*. 2017 Mar 14; 114(11):E2166-E2175. Doi: 10.1073/pnas.1613916114.

Hagan I.M. The spindle pole body plays a key role in controlling mitotic commitment in the fission yeast Schizosaccharomyces Pombe. *Biochem Soc Trans.* 2008 Oct; 36(Pt 5):1097-101. Doi: 10.1042/BST0361097.

Hachet V., C. Canard and P. Gönczy. Centrosomes promote timely mitotic entry in *C. elegans* embryos. *Dev Cell*. 2007 Apr; 12(4):531-41. Doi: 10.1016/j.devcel.2007.02.015.

Hirano Y., Y. Kinugasa, H. Asakawa, Y. Chikashige, C. Obuse, T. Haraguchi and Y. Hiraoka. Lem2 is retained at the nuclear envelope through its interaction with Bqt4 in fission yeast. *Genes Cells.* 2018 Mar; 23(3):122-135. Doi: 10.1111/gtc.12557.

Hiraoka Y., H. Maekawa, H. Asakawa, Y. Chikashige, T. Kojidani, H. Osakada, A. Matsuda and T. Haraguchi. Inner nuclear membrane protein Ima1 is dispensable for intranuclear positioning of centromeres. *Genes Cells.* 2011 Oct; 16(10):1000-11. Doi: 10.1111/j.1365-2443.2011.01544.x.

Hou H., Z. Zhou, Y. Wang, J. Wang, S.P. Kallgren, T. Kurchuk, E.A. Miller, F. Chang and S. Jia. Csi1 links centromeres to the nuclear envelope for centromere clustering. *J Cell Biol*. 2012 Nov 26; 199(5):735-44. Doi: 10.1083/jcb.201208001.

Hu C., H. Inoue, W. Sun, Y. Takashita, Y. Huang, Y. Xu, J. Kanoh and Y. Chen. Structural insights into chromosome attachment to the nuclear envelope by an inner nuclear membrane protein Bqt4 in fission yeast. *Nucleic Acids Res.* 2019 Feb 20; 47(3):1573-1584. Doi: 10.1093/nar/gky1186.

Klutstein M. and J.P. Cooper. The chromosomal courtship dance-homolog pairing in early meiosis. *Curr Opin Cell Biol.* 2014 Feb; 26:123-31. Doi: 10.1016/j.ceb.2013.12.004.

Kollman J.M., A. Merdes, L. Mourey and D.A. Agard. Microtubule nucleation by γ-tubulin complexes. *Nat Rev Mol Cell Biol.* 2011 Oct 12; 12(11):709-21. Doi: 10.1038/nrm3209.

Lenart P., M. Petronczki, M. Steegmaier, B. Di Fiore, J.J. Lipp, M. Hoffmann, W.J. Rettig, N. Kraut and J.M. Peters. The small-molecule inhibitor BI 2536 reveals novel insights into mitotic roles of polo-like kinase 1. *Curr Biol.* 2007 Feb 20; 17(4):304-15. Doi: 10.1016/j.cub.2006.12.046.

Leverson J.D., H.K. Huang, S.L. Forsburg and T. Hunter. The Schizosaccharomyces Pombe aurora-related kinase Ark1 interacts with the inner centromere protein Pic1 and mediates chromosome segregation and cytokinesis. *Mol Biol Cell.* 2002 Apr; 13(4):1132-43. Doi: 10.1091/mbc.01-07-0330.

MacIver F.H., K. Tanaka, A.M. Robertson and I.M. Hagan. Physical and functional interactions between polo kinase and the spindle pole component Cut12 regulate mitotic commitment in S. pombe. *Genes Dev.* 2003 Jun 15; 17(12):1507-23. Doi: 10.1101/gad.256003.

Miki F., A Kurabayashi, Y. Tange, K Okazaki, M Shimanuki and O Niwa. Two-hybrid search for proteins that interact with Sad1 and Kms1, two membrane-bound components of the spindle pole body in fission yeast. *Mol. Genet. Genomics*. 2004 Jan; 270(6):449-61. Doi: 10.1007/s00438-003-0938-8.

Mulvihill D.P., J. Peterson, H. Ohkura, D.M. Glover and I.M. Hagan. Plo1 kinase recruitment to the spindle pole body and its role in cell division in Schizosaccharomyces pombe. *Mol Biol Cell*. 1999 Aug; 10(8):2771-85. Doi: 10.1091/mbc.10.8.2771.

Nigg E.A. Centrosome aberrations: cause or consequence of cancer progression? *Nat Rev Cancer*. 2002 Nov; 2(11):815-25. Doi: 10.1038/nrc924.

Nurse P. and P. Thuriaux. Regulatory genes controlling mitosis in the fission yeast Schizosaccharomyces Pombe. *Genetics.* 1980 Nov; 96(3):627-37. PMID: 7262540.

Ohkura H., I.M. Hagan and D.M. Glover. The conserved Schizosaccharomyces Pombe kinase plo1, required to form a bipolar spindle, the actin ring, and septum, can drive septum formation in G1 and G2 cells. *Genes Dev.* 1995 May 1; 9(9):1059-73. Doi: 10.1101/gad.9.9.1059.

Paddy M.R., H. Saumweber, D.A. Agard and J.W. Sedat. Time-resolved, *in vivo* studies of mitotic spindle formation and nuclear lamina breakdown in Drosophila early embryos. *J Cell Sci*. 1996 Mar; 109(Pt 3):591-607.

Petersen J., J. Paris, M. Willer, M. Philippe and I.M. Hagan. The S. pombe aurora-related kinase Ark1 associates with mitotic structures in a stage dependent manner and is required for chromosome segregation. *J Cell Sci.* 2001 Dec; 114(Pt 24):4371-84. PMID: 11792803.

Portier N., A. Audhya, P.S. Maddox, R.A. Green, A. Dammermann, A. Desai and K. Oegema. A microtubule-independent role of centrosomes and aurora a in nuclear envelope breakdown. *Dev Cell*. 2007 Apr; 12(4):515-29. Doi: 10.1016/j.devcel.2007.01.019.

Rahman M.M., M. Munzig, K Kaneshiro, B. Lee, S. Strome, T. Muller-Reichert and O. Cohen-Fix. Caenorhabditis elegans polo-like kinase PLK-1 is required for merging parental genomes into a single nucleus. *Mol Biol Cell.* 2015 Dec 15; 26(25):4718-35. Doi: 10.1091/mbc.E15-04-0244.

Rüthnick D., A. Neuner, F. Dietrich, D. Kirrmaier, U. Engel, M. Knop and E. Schiebel. Characterization of spindle pole body duplication reveals a regulatory role for nuclear pore complexes. 2017 Aug 7; 216(8):2425-2442. Doi: 10.1083/jcb.201612129.

Steglich B., G.J. Filion, B. van Steensel and K. Ekwall. The inner nuclear membrane proteins Man1 and Ima1 link to two different types of chromatin at the nuclear periphery in S. pombe. *Nucleus.* 2012 Jan-Feb; 3(1):77-87. Doi: 10.4161/nucl.18825.

Swaffer M.P., A.W. Jones, H.R. Flynn, A.P. Snijders and P. Nurse. Quantitative phosphoproteomics reveals the signaling dynamics of cell-cycle kinases in the fission yeast Schizosaccharomyces Pombe. *Cell Rep.* 2018 Jul 10; 24(2):503-514. Doi: 10.1016/j.celrep.2018.06.036.

Takahashi K., E.S. Chen and M. Yanagida. Requirement of Mis6 centromere connector for localizing CENP-A-like protein in fission yeast. *Science.* 2000 Jun 23; 288(5474):2215-9. Doi: 10.1126/science.288.5474.2215.

Tallada V.A., K. Tanaka, M. Yanagida and I.M. Hagan. The S. pombe mitotic regulator Cut12 promotes spindle pole body activation and integration into the nuclear envelope. *J Cell Biol.* 2009 Jun 1; 185(5):875-88. Doi: 10.1083/jcb.200812108.

Tamm T., A. Grallert, E.P. Grossman, I. Alvarez-Tabares, F.E. Stevens and I.M. Hagan. Brr6 drives the Schizosaccharomyces Pombe spindle pole body nuclear envelope insertion/extrusion cycle. *J Cell Biol.* 2011 Oct 31; 195(3):467-84. Doi: 10.1083/jcb.201106076.

Tomita K. and J.P. Cooper. The telomere bouquet controls the meiotic spindle. *Cell.* 2007 Jul 13; 130(1):113-26. Doi: 10.1016/j.cell.2007.05.024.

Uzawa S., F. Li, Y. Jin, K.L. McDonald, M.B. Braunfeld, D.A. Agard and W.Z. Cande. Spindle pole body duplication in fission yeast occurs at the G1/S boundary but maturation is blocked until exit from S by an event downstream of cdc10+. *Mol Biol Cell.* 2004 Dec; 15(12):5219-30. Doi: 10.1091/mbc.e04-03-0255.

Varberg J.M., J.M. Gardner, S. McCroskey, S. Saravanan, W.D. Bradford and S.L. Jaspersen. High-throughput identification of nuclear envelope protein interactions in Schizosaccharomyces pombe using an arrayed membrane yeast-two hybrid library. *G3 (Bethesda)*. 2020 Oct 27; g3.401880.2020. Doi: 10.1534/g3.120.401880.

Wälde S. and M.C. King. The KASH protein Kms2 coordinates mitotic remodeling of the spindle pole body. *J Cell Sci.* 2014 Aug 15; 127(Pt 16):3625-40. Doi: 10.1242/jcs.154997.

West R.R., E.V. Vaisberg, R. Ding, P. Nurse and J.R. McIntosh. Cut11(+): A gene required for cell cycle-dependent spindle pole body anchoring in the nuclear envelope and bipolar spindle formation in Schizosaccharomyces Pombe. *Mol Biol Cell.* 1998 Oct; 9(10):2839-55. Doi: 10.1091/mbc.9.10.2839.

Wu J. and A. Akhmanova. Microtubule-organizing centers. *Annu Rev Cell Dev Biol.* 2017 Oct 6; 33:51-75. Doi: 10.1146/annurev-cellbio-100616-060615.

Table S1. Yeast Strains.

Strain	Genotype	Source/Reference	Figure
fySLJ308	h? *sad1-GFP-KanMX6, ppc89-mCherry-NatMX6, cdc25.22, leu1-32, ura4-D18, his3-D1*	Bestul et al. (2017)	Fig. 1A, B Fig. 3A, S1A Fig. 6A-C
fySLJ313	h? *cut12-GFP-KanMX6, ppc89-mCherry-NatMX6, cdc25.22, leu1-32, ura4-D18*	This study	Fig. 1A, B Fig. 6A, B, D
fySLJ314	h? *KanMX6-41nmt1-GFP-kms2, ppc89-mCherry-NatMX6, cdc25.22, leu1-32, ura4-D18, his3-D1*	Bestul et al. (2017)	Fig. 1A, B
fySLJ400	h? *cut11-GFP-Ura4+, ppc89-mCherry-NatMX6, cdc25.22, leu1-32, ura4-D18*	This study	Fig. 1A, B
fySLJ228	h+ *cut12-GFP-KanMX6, ppc89-mCherry-NatMX6, ade6-M216, his-D1, leu1-32, ura4-D18*	Bestul et al. (2017)	Fig. 1C
fySLJ492	h? *cut12-GFP-KanMX6, ppc89-mCherry-NatMX6, sad1.1, leu1-32, ura4-D18*	This study	Fig. 1C
fySLJ282	h- *KanMX6-41nmt1-GFP-kms2, ppc89-mCherry-NatMX6, ade6-M210, leu1-32, ura4-D18, his3-D1*	Bestul et al. (2017)	Fig. 1C
fySLJ493	h? *KanMX6-41nmt1-GFP-kms2, ppc89-mCherry-NatMX6, sad1.1, leu1-32, ura4-D18*	This study	Fig. 1C
fySLJ450	h+ *cut11-GFP-Ura4+, ppc89-mCherry-NatMX6, leu1-32, ura4-D18*	This study	Fig. 1C
fySLJ490	h? *cut11-GFP-Ura4+, ppc89-mCherry-NatMX6, sad1.1, leu1-32, ura4-D18*	This study	Fig. 1C
fySLJ237	h+ *sad1-GFP-KanMX6, ppc89-mCherry-NatMX6, ade6-M216, leu1-32, ura4-D18, his3-D1*	Bestul et al. (2017)	Fig. 1D
fySLJ328	h? *sad1-GFP-KanMX6, ppc89-mCherry-NatMX6, cut11.1, leu1-32, ura4-D18*	This study	Fig. 1D
fySLJ324	h? *sad1-GFP-KanMX6, ppc89-mCherry-NatMX6, cut11.1, leu1-32, ura4-D18*	This study	Fig. 1D
fySLJ494	h? *sad1-GFP-KanMX6, ppc89-mCherry-HygMX6, NatMX6-81nmt1-HA-Kms2-KanMX6, leu1-32, ura4-D18*	This study	Fig. 1D
fySLJ941		This study	Fig. 2A, B

fySLJ923	h? *pREP3X-SV40NLS-GFP-lacZ, ppc89-mCherry-NatMX6, leu1-32, ura4-D18*	This study	Fig. 2A, B
fySLJ985	h? *pREP3X-SV40NLS-GFP-lacZ, ppc89-mCherry-NatMX6, sad1.1, leu1-32, ura4-D18*	This study	Fig. 2A, B
fySLJ943	h? *pREP3X-SV40NLS-GFP-lacZ, ppc89-mCherry-NatMX6, cut12.1, leu1-32, ura4-D18*	This study	Fig. 2A, B
fySLJ942	h? *pREP3X-SV40NLS-GFP-lacZ, ppc89-mCherry-NatMX6, cut11.1, leu1-32, ura4-D18*	This study	Fig. 2A, B
fySLJ922	h? *pREP3X-SV40NLS-GFP-lacZ, ppc89-mCherry-NatMX6, brr6.ts8, leu1-32, ura4-D18*	This study	Fig. 2A, B
fySLJ1070	h? *pREP3X-SV40NLS-GFP-lacZ, ppc89-mCherry-HygMX6, NatMX6-81nmt1-HA-Kms2-KanMX6, leu1-32, ura4-D18*	This study	Fig. S1B
fySLJ698	h? *mis6-GFP-KanMX6, sad1-mCherry-NatMX6, cdc25.22, leu1-32, ura4-D18*	This study	Fig. S1C, D
fySLJ699	h? *sad1-GFP-NatMX6, ppc89-mCherry-HygMX6, lem2Δ::KanMX6, leu1-32, ura4-D18*	This study	Fig. S1C, D
fySLJ700	h? *sad1-GFP-NatMX6, ppc89-mCherry-HygMX6, nur1Δ::KanMX6, leu1-32, ura4-D18*	This study	Fig. S1C, D
fySLJ701	h? *sad1-GFP-NatMX6, ppc89-mCherry-HygMX6, bqt4Δ::KanMX6, leu1-32, ura4-D18*	This study	Fig. S1C, D
fySLJ752	h? *sad1-GFP-NatMX6, ppc89-mCherry-HygMX6, cmp7Δ::KanMX6, leu1-32, ura4-D18*	This study	Fig. S1C, D
fySLJ1063	h? *sad1-GFP-NatMX6, ppc89-mCherry-HygMX6, ima1Δ::KanMX6, leu1-32, ura4-D18*	This study	Fig. 3B
fySLJ981	h? *csi1-GFP-KanMX6, sad1-mCherry-NatMX6, cdc25.22, leu1-32, ura4-D18*	This study	Fig. 3A
fySLJ939	h? *csi1-GFP-KanMX6, ppc89-mCherry-NatMX6, cdc25.22, leu1-32, ura4-D18*	This study	Fig. 3C
fySLJ1035	h- *csi1-GFP-KanMX6, ppc89-mCherry-NatMX6, leu1-32, ura4-D18*	This study	Fig. 3C
fySLJ1036	h? *csi1-GFP-KanMX6, ppc89-mCherry-NatMX6, sad1.1, leu1-32, ura4-D18*	This study	Fig. 3C

fySLJ1037	h? *csi1-GFP-KanMX6, ppc89-mCherry-NatMX6, cut12.1, leu1-32, ura4-D18*	This study	Fig. 3C
fySLJ1055	h? *csi1-GFP-KanMX6, ppc89-mCherry-NatMX6, cut11.1, leu1-32, ura4-D18*	This study	Fig. 3C
fySLJ761	h? *csi1-GFP-KanMX6, ppc89-mCherry-HygMX6, NatMX6-81nmt1-HA-Kms2-KanMX6, leu1-32, ura4-D18*	This study	Fig. 3D, E
fySLJ1039	h? *sad1-GFP-NatMX6, ppc89-mCherry-HygMX6, csi1Δ::KanMX6, leu1-32, ura4-D18*	This study	Fig. 3D, E
fySLJ590	h? *sad1-GFP-NatMX6, ppc89-mCherry-NatMX6, lem2Δ::KanMX6, csi1Δ::HygMX6, leu1-32, ura4-D18*	This study	Fig. S2A
fySLJ1062	h? *lem2-GFP-KanMX6, ppc89-mCherry-NatMX6, cdc25.22, leu1-32, ura4-D18*	This study	Fig. S2B
fySLJ577	h? *cut11-GFP-KanMX6, lem2-mCherry-HygMX6, cdc25.22, leu1-32, ura4-D18*	This study	Fig. S2C
fySLJ586	h+ *lem2-GFP-KanMX6, ppc89-mCherry-NatMX6, leu1-32, ura4-D18*	This study	Fig. S2C
fySLJ703	h? *lem2-GFP-KanMX6, ppc89-mCherry-NatMX6, sad1.1, leu1-32, ura4-D18*	This study	Fig. S2C
fySLJ721	h? *lem2-GFP-KanMX6, ppc89-mCherry-HygMX6, NatMX6-81nmt1-HA-Kms2-KanMX6, leu1-32, ura4-D18*	This study	Fig. S2C
fySLJ722	h? *lem2-GFP-KanMX6, ppc89-mCherry-NatMX6, cut11.1, leu1-32, ura4-D18*	This study	Fig. S2C
JCF8287	h? *lem2-GFP-KanMX6, ppc89-mCherry-NatMX6, cut12.1, leu1-32, ura4-D18*	Fernandez-Alvarez et al. (2016)	Fig. 4A, B
fySLJ466	h90 *sad1.2-GFP-KanMX6, ade6-M216*	This study	Fig. 4A, B
fySLJ1016	h+ *sad1.2-GFP-KanMX6, ppc89-mCherry-NatMX6, leu1-32, ura4-D18*	This study	Fig. 4A, B
JCF14183	h? *sad1.2-GFP-KanMX6, ppc89-mCherry-NatMX6, csi1Δ::HygMX6, leu1-32, ura4-D18*	Fernandez-Alvarez et al. (2016)	Fig. 4C-E Fig. 6F, G
fySLJ1041	h- *ade6-M216 sad1.2-mTurq2-NatMX6, bleMX6-nmt3X-bqt1-GBP-mCherry:HygMX6, Pnda3-mCherry-atb2:aur1R, Mis6-GFP:kanMX6*	This study	Fig. 4C-E

KYG8562	h? *sad1.2-mTurq2-NatMX6, bleMX6-nmt3X-bqt1-GBP-mCherry:HygMX6*	K. Gould Lab	Fig. 5A, B
fySLJ605	h+ *ark1-T7-KanMX6, leu1-32, ura4-D18*	This study	Fig. 5A, B
KS7836	h? *ark1-T7-KanMX6, sad1-GFP-NatMX6, ppc89-mCherry-HygMX6, leu1-32, ura4-D18*	K. Sawin Lab	Fig. 5A, B
fySLJ606	h- *cdc2-asM17-Bsd, leu1-32, ura4-D18*	This study	Fig. 5A, B
KYG808	h? *cdc2-asM17-Bsd, sad1-GFP-KanMX6, ppc89-mCherry-NatMX6, leu1-32, ura4-D18*	K. Gould Lab	Fig. 5A, B
fySLJ604	h- *plo1-24c, leu1-32, ura4-D18*	This study	Fig. 5A, B
AP2828	h? *plo1-24c, sad1-GFP-KanMX6, ppc89-mCherry-NatMX6, leu1-32, ura4-D18*	A. Paoletti Lab	Fig. 5C
fySLJ986	h+ *plo1-GFP-KanMX6, leu1-32, ura4+*	This study	Fig. 5C
fySLJ1096	h? *plo1-GFP-KanMX6, ppc89-mCherry-NatMX6, cdc25.22, leu1-32, ura4-D18*	This study	Fig. 5C
IJ10368	h? *plo1-GFP-KanMX6, Sad1-mCherry-NatMX6, cdc25.22, leu1-32, ura4-D18*	I. Hagan Lab	Fig. 6A-G
fySLJ754	h- *plo1-as8-Ura4+, leu1-32, ura4-D18*	This study	Fig. 6A-C
fySLJ1067	h? *sad1-GFP-KanMX6, ppc89-mCherry-HygMX6, cdc25.22, plo1-as8-Ura4+, leu1-32, ura4-D18*	This study	Fig. 6A, B, D
fySLJ824	h? *cut12-GFP-KanMX6, ppc89-mCherry-NatMX6, cdc25.22, plo1-as8-Ura4+, leu1-32, ura4-D18*	This study	Fig. 6A, E
fySLJ859	h? *pREP3X-SV40NLS-GFP-lacZ, ppc89-mCherry-NatMX6, cdc25.22, leu1-32, ura4-D18*	This study	Fig. 6A, E
fySLJ1095	h? *pREP3X-SV40NLS-GFP-lacZ, ppc89-mCherry-NatMX6, cdc25.22, plo1-as8-Ura4+, leu1-32, ura4-D18*	This study	Fig. 6F, G
	h? *sad1.2-mTurq2-NatMX6, bleMX6-nmt3X-bqt1-GBP-mCherry-HygMX6, Mis6-GFP-KanMX6, plo1.as8-Ura4+, ura4-D18*		